

Syracuse University

**SURFACE**

---

Theses - ALL

---

December 2017

## Cell laden hydrogel microspheres using 3D printed microfluidics

Sanika Nitin Suvarnapathaki  
*Syracuse University*

Follow this and additional works at: <https://surface.syr.edu/thesis>



Part of the [Engineering Commons](#)

---

### Recommended Citation

Suvarnapathaki, Sanika Nitin, "Cell laden hydrogel microspheres using 3D printed microfluidics" (2017).  
*Theses - ALL*. 188.  
<https://surface.syr.edu/thesis/188>

This Thesis is brought to you for free and open access by SURFACE. It has been accepted for inclusion in Theses - ALL by an authorized administrator of SURFACE. For more information, please contact [surface@syr.edu](mailto:surface@syr.edu).

## **Abstract**

Current tissue engineering therapies use macro-scale three dimensional (3D) scaffolds to treat tissue defects surgically. Uneven cell seeding and oxygen and media perfusion cause low cell viability in these macro-scale scaffolds. Microencapsulation, a technique of encapsulating cells in biocompatible polymers or hydrogels, has the potential to address these key issues, and therefore this technology has been used for numerous healthcare applications over the last two decades. Cell microencapsulation in hydrogels that mimic the tissue physiology and biochemistry has made it possible to use natural hydrogels like gelatin methacrylate (GelMA) to encapsulate cells in microspheres inside an oil emulsion, to serve as micron scale scaffolds to encapsulate cells for tissue engineering applications. Cell microencapsulation, however, has challenges with respect to the number of cell laden microspheres that can be achieved repeatedly with a consistent cell density per microsphere and their ability to achieve and maintain a high cell viability. This is the major impediment to the clinical translation of cell microencapsulation to treat tissue defects without surgery. In this work, cells were encapsulated within GelMA microspheres, ranging 30-250 micrometers in diameter using a 3D printing and replica casting-molding approach. It is a non-clean room fabrication approach and hence a relatively inexpensive universal platform to encapsulate cells. Rheological properties of varying GelMA concentration were used to identify optimal concentration, flow rates of the GelMA and oil phases and the pressures required to achieve the desired size of microspheres with high repeatability. The success of this approach is demonstrated by high cell viability observed in the *in vitro* results. The use of 3D printing makes the fabrication of this microfluidic chip easy,

inexpensive and accessible to biological researchers, and as a result, help lower the barrier of entry to the field of microencapsulation.

**CELL LADEN HYDROGEL MICROSPHERES USING 3D PRINTED  
MICROFLUIDICS**

By

**SANIKA SUVARNAPATHAKI**

B.E. Biomedical Engineering, University of Mumbai, 2015

**THESIS**

Submitted in partial fulfillment of the requirements for the  
degree of Master of Science in Bioengineering

Syracuse University

December 2017

Copyright © Sanika Suvarnapathaki 2017

All Rights Reserved

*I want to dedicate this work to my parents Dr. Sujata and Nitin Suvarnapathaki, my godparents Dr. Ruta Sahasrabudhe and Dr. Nikhil Bhagwat, my PI Dr. Pranav Soman and entire Soman lab for their constant love, support and encouragement that drives my inspiration to pursue research*

## **Acknowledgements**

I want to express my deepest gratitude to my PI Dr. Pranav Soman, for his constant guidance and encouragement to help this work become possible. I am grateful to the entire Soman research group for their kindness, encouragement and honest co-operation during my long experiments.

I want to sincerely thank Stephen Sawyer for his guidance and encouragement throughout the cell experiments that helped us run the experiments with no contamination and maximum efficiency. I want to thank the undergraduate students Andrew Ramos, Sarah Venn and Shannon McLoughlin who assisted me on this project, helping me with the elaborate set ups with utmost patience. I thank my colleague Rafael Ramos for training me on GelMA synthesis and the rheometer to be able to get my rheological data. I want to thank Dr. Jay Henderson for his guidance and encouragement during my lab transition from the Esch to Soman group. I thank Dr. Eric Finklestein for providing training on multiple equipment at SBI.

I want to sincerely thank the NAPPI Foundation for funding this project throughout. I also want to thank Cornell NanoBiotechnology Center (NBTC Facility), Cornell University for assisting me with 3D printing of the device Mold. I want to thank Prof. Shalabh C. Maroo's lab in Life Sciences Complex, Department of Mechanical and Aerospace Engineering, for allowing me to use their Plasma cleaner to bond our PDMS chips to glass. I want to thank Mr. Tom Corso from Corsolutions, LLC for helping us service and maintain our pneu wave dual channel microfluidic pumps. I also want to thank Syracuse Biomaterials Institute for housing our experiments. I thank the faculty and staff in the department for their help in direct or indirect ways. Finally, I owe an ocean of gratitude to my parents, family and friends for always believing in me.

# Table of Contents

<b>List of Tables .....</b>	<b>ix</b>
<b>List of Schemes.....</b>	<b>x</b>
<b>List of Figures .....</b>	<b>xii</b>
<b>Chapter 1 Introduction .....</b>	<b>01</b>
1.1 Introduction to tissue engineering.....	01
1.2 Overview of current challenges in tissue engineering.....	02
1.3 Importance of cell microencapsulation .....	04
1.4 Existing technologies for microencapsulation and drawbacks .....	05
1.5 Goal of thesis work.....	10
<b>Chapter 2 Experimental Design .....</b>	<b>11</b>
2.1 Materials and Methods.....	11
2.1.1 GelMA Synthesis protocol.....	11
2.1.2 Device fabrication .....	12
2.1.2.1 Design and fabrication of the 3D printed mold.....	12
2.1.3 Set up.....	14
2.2 Non-cell emulsion experiments.....	15
2.2.1 Viscometric characterization.....	16
2.2.2 Rheological characterization.....	16
2.2.3 Injection experiments.....	17
2.3 Cell Experiments.....	18
2.3.1 Step 1:Component Sterilization.....	18
2.3.2 Step 2:Making GelMA prepolymer solution.....	18
2.3.3 Step 3:Making the cell solution.....	19
2.3.3.1 Cell solution protocol.....	19
2.3.3.2 Osteosarcoma Cell culture.....	20
2.3.4 Step 4:The encapsulation process.....	20
2.3.5 Staining Study.....	21
2.3.5.1 Live/dead staining.....	21
<b>Chapter 3 Results and Discussion.....</b>	<b>23</b>
3.1 Non-cell GelMA microsphere synthesis.....	23



3.2 Characterization of material properties.....	25
3.3 Cell encapsulation experiments.....	29
<b>Chapter 4 Discussion, Conclusion and future scope.....</b>	<b>35</b>
4.1 Discussion.....	35
4.2 Research approach.....	35
4.2.1 Fabrication approach.....	37
4.2.2 Cell viability in microencapsulation.....	38
4.2.3 Sample collection efficiency and microsphere size repeatability.....	39
4.2.4 Repeatability of number of cells encapsulated per microsphere.....	40
4.3 Conclusions.....	43
 <b>Appendix A .....</b>	 <b>44</b>
<b>Bibliography .....</b>	<b>52</b>
<b>Vita ....</b>	<b>56</b>

## List of Tables

<b>Table 1:</b>	UV crosslinking time observed for microspheres made using different (w/v) GelMA concentrations.....	<b>23</b>
<b>Table 2:</b>	Different mean microsphere sizes achieved using different flow rates.....	<b>25</b>
<b>Table 3:</b>	Table representing the number of microspheres per unit emulsion volume .....	<b>29</b>
<b>Table 4:</b>	Average number of cells encapsulated per microsphere of different mean diameters.....	<b>31</b>
<b>Table 5:</b>	Table representing average percentage viability and corresponding standard deviation .....	<b>33</b>
<b>Table 6:</b>	Average percentage increase in mean diameter of microspheres of different sizes (Swelling behavior) .....	<b>48</b>
<b>Table 7:</b>	Standard deviations in the corresponding percentage increase in mean sphere size.....	<b>49</b>
<b>Table 8:</b>	Percentage viability observed for n=10 emulsion samples for Day 1, Day 7, Day 14 and Day 21.....	<b>49</b>
<b>Table 9:</b>	One way ANOVA analysis table.....	<b>50</b>
<b>Table 10:</b>	Bonferroni pair wise tests comparison of percentage viability as observed between different time points.....	<b>51</b>

## **List of Schemes**

<b>Scheme 1:</b>	Basic concept of tissue engineering therapy.....	<b>02</b>
<b>Scheme 2:</b>	Cell encapsulation application in tissue engineering therapy.....	<b>04</b>
<b>Scheme 3:</b>	Existing technology for cell microencapsulation.....	<b>06</b>
<b>Scheme 4:</b>	Microfluidic devices used for cell encapsulation.....	<b>08</b>
<b>Scheme 5:</b>	Sketch representing final microfluidic chip dimensions.....	<b>46</b>

## List of Figures

<b>Figure 1:</b> (A) 2D front view and (B) 3D oblique view of the channel dimensions.....	<b>13</b>
<b>Figure 2:</b> (A) 3D printed mold and (B) Microfluidic device after replica molding and plasma bonding.....	<b>14</b>
<b>Figure 3:</b> Experimental set up.....	<b>15</b>
<b>Figure 4:</b> (A) GelMA microspheres $35\mu\text{m}$ in mean diameter made from 8%(w/v) GelMA and (B) Table 1 representing UV crosslinking time for crosslinking microspheres made from different (w/v) concentration of GelMA.....	<b>23</b>
<b>Figure 5:</b> (A) Table 2 different mean microsphere sizes achieved using different flow rate and (B) Representative images of 50,100 and $150\mu\text{m}$ microspheres.....	<b>25</b>
<b>Figure 6:</b> (A) Viscosity profiles of different (w/v) GelMA concentration prepolymer solutions and (B) Storage and loss moduli for 8% (w/v) GelMA slab.....	<b>26</b>
<b>Figure 7:</b> (A) Swelling profiles: %increase in mean microsphere diameter as observed with time and (B) Represents the before and after swelling images of 50,100 and $150\mu\text{m}$ mean microsphere sizes.....	<b>27</b>
<b>Figure 8:</b> (A) Before and (B) After injection image of $100\mu\text{m}$ GelMA microspheres through a 20-gauge needle.....	<b>28</b>
<b>Figure 9:</b> (A) Graph and (B) Table 3. Representing average number of microspheres per $\mu\text{l}$ of emulsion volume.....	<b>29</b>
<b>Figure 10:</b> Single microsphere cell encapsulation images. $100\mu\text{m}$ sphere with cells encapsulated (A) in media and (B) in perfluorodecalin oil.....	<b>30</b>
<b>Figure 11:</b> (A) Table 4 and (B) Graph representing the average number of cells encapsulated per microsphere for different mean microsphere diameters.....	<b>31</b>

<b>Figure 12:</b> (i) Day 1, (ii) Day 7, (iii) Day 14 and (iv) Day 21 viability (A) Percentage viability as quantified on Day 1, Day 7, Day 14 and Day 21 and (B) Table 5 representing average percentage viability and corresponding standard deviations.....	<b>33</b>
<b>Figure 13:</b> Fluores brite fluorescence beads encapsulated in an oil emulsion.....	<b>44</b>
<b>Figure 14:</b> Degradation of a microspheres as observed on (i) Day 27 and (ii) Day 29 respectively.....	<b>45</b>
<b>Figure 15:</b> (A) Before and (B) After images 20x from injection of 100µm 8%w/v GelMA microspheres using a 23-gauge needle (Scale bar: 500 µm) .....	<b>47</b>
<b>Figure 16:</b> (A) Before and (B) After injection 5x 20µl emulsion of 100µm of 8%w/v GelMA using a 23-gauge needle (Scale bar: 500 µm) .....	<b>47</b>

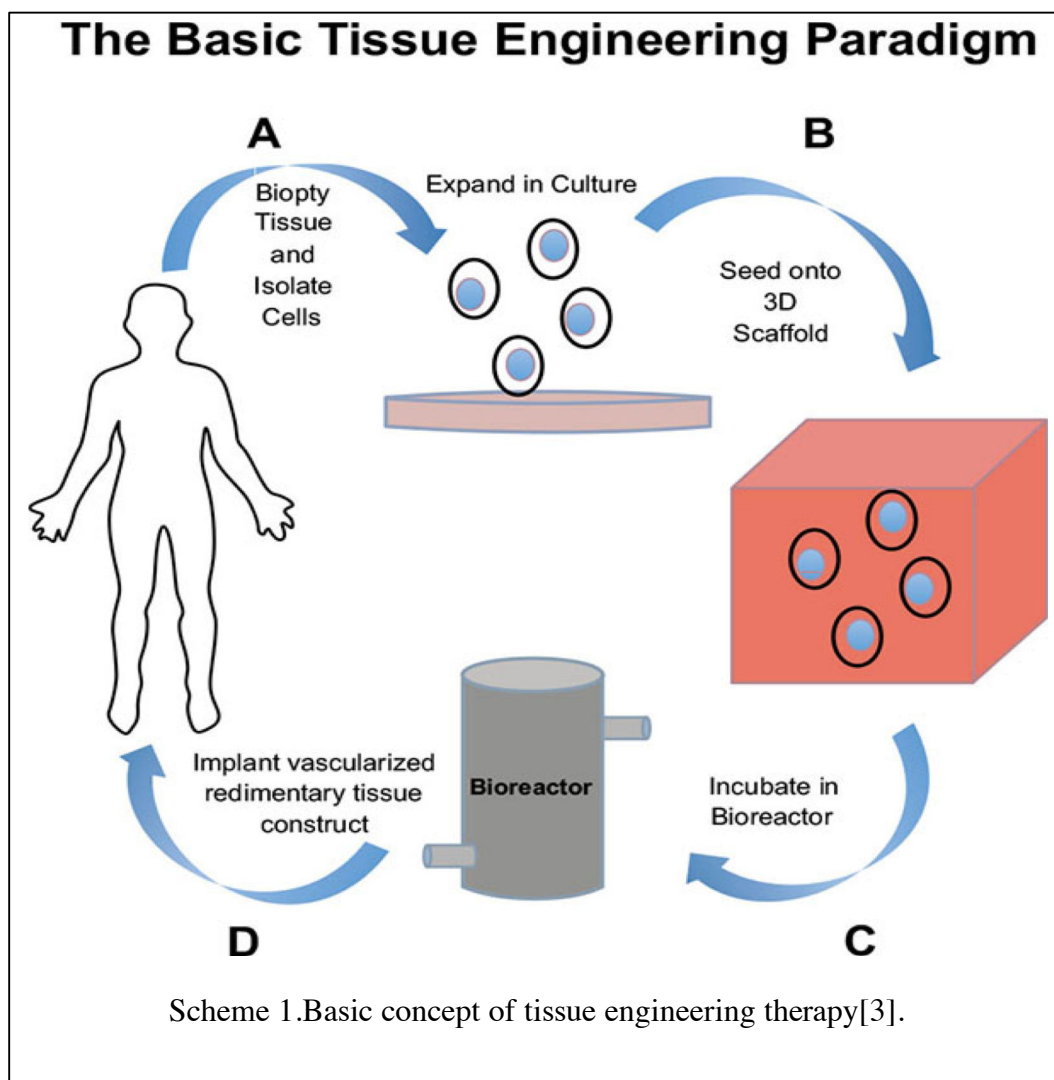
## **Chapter 1: Introduction**

### **Scope**

This section comprises of an overview of the current challenges in fabrication techniques used widely in clinical settings for tissue engineering therapy.

### **1.1 Introduction to tissue engineering**

Tissue engineering is a technique of using organ specific cells and seeding them onto support structures or scaffolds made out of biomaterials. These may be infused with bioactive factors that assist the viability, differentiation, and proliferation of cells when surgically implanted into the patient to develop functional organs[1]. Scaffolds or support structures are essential to hold the cells in a structure inside the body and also to provide a surface of attachment for the cells to grow and proliferate. Scheme 1 shows the basic concept of tissue engineering therapy. Stem cells are usually taken from a patient by a biopsy and they are cultured, expanded and seeded onto the macro scale (mm or cm or inch size) three dimensional (3D) scaffolds. These scaffolds are incubated in bioreactors that are units that help perfuse cell media, oxygen, and bioactive factors to assist cell viability, proliferation, and integration of blood supply or vascularization. It is important that the scaffolds are vascularized to ensure that the cells stay alive in the scaffold. This incubated scaffold is then surgically implanted into the patient where it should integrate with the host as the cells differentiate into the specific functional tissues. Most of the approaches used in clinical tissue engineering therapy involve the use of macro scale scaffolds for seeding cells. These macro scale approaches involve two main challenges (i) uneven cell seeding throughout the 3D scaffold and (ii) inadequate oxygen and media perfusion throughout the scaffolds which could affect cell viability upon implantation[2].

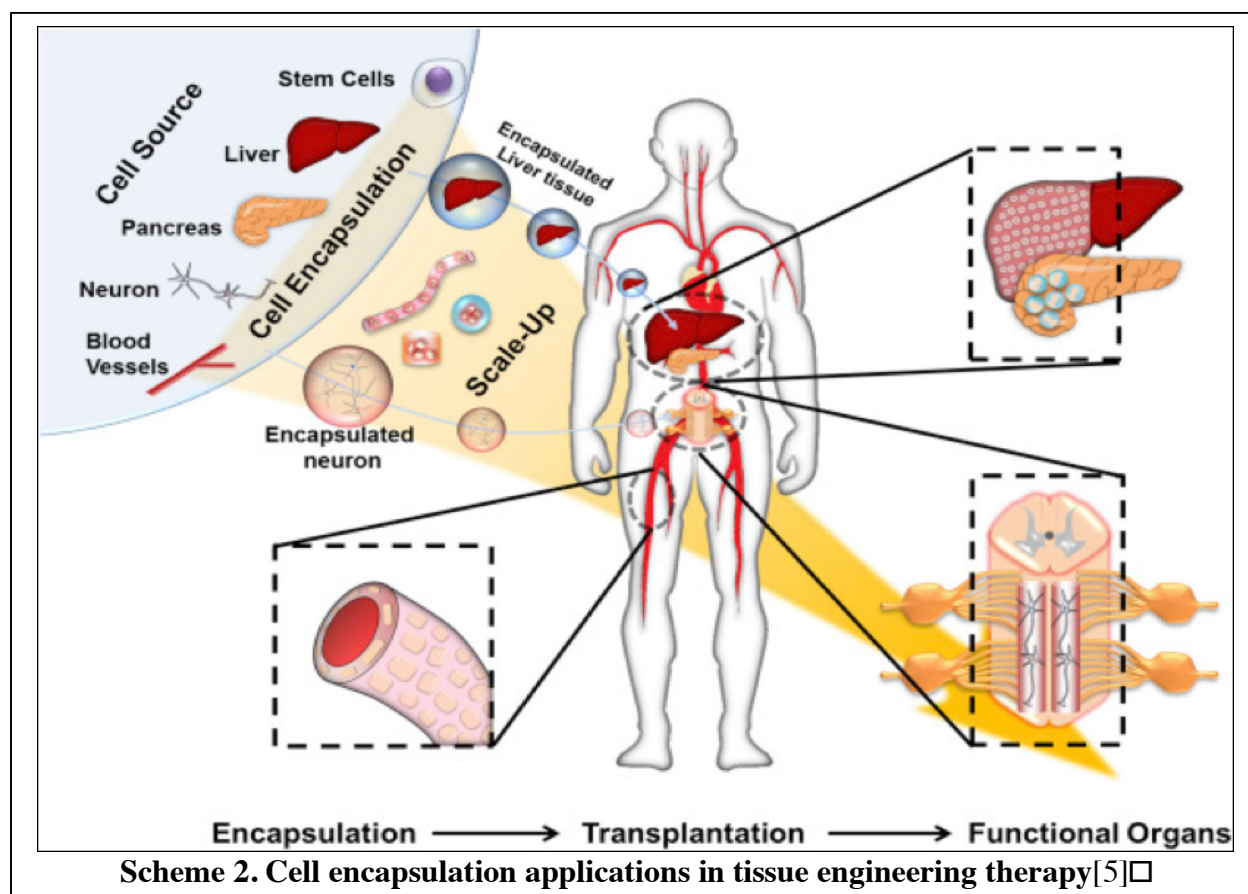


## 1.2 Overview of cell encapsulation in tissue engineering and current challenges.

Seeding cells on scaffolds have challenges with achieving uniform cell distribution throughout the scaffold. The idea of cell encapsulation is to encapsulate cells in spheres made out of biocompatible polymers or hydrogels and seed these cell laden spheres on a three-dimensional (3D) scaffold. Cell encapsulation has proven to be an effective cell seeding technique to ensure even cell seeding throughout the 3D scaffold volume [3]. This scaffold can then be surgically implanted in the patient. The function of a scaffold is to degrade with time while holding the

encapsulated cells within the organ's macro structure allowing them to differentiate and proliferate [4]. Cell encapsulation in hydrogels has proved to be an effective cell encapsulation approach [3]. As shown in Scheme 2, tissue engineering functional organs use cell encapsulation technologies to ensure even cell distribution and density throughout the scaffold volume. Stem cells specific to the tissue type are taken from patients and are encapsulated in spheres made out of biodegradable polymers or hydrogels that mimic the *in vivo* environment. A large number of these cell laden spheres are then seeded on scaffolds and this helps ensure a better 3D distribution of cells throughout the scaffold volume. Since the cells are encapsulated in spheres, stacking multiple such cell laden spheres give a natural porosity to the macro structure of the scaffold. This allows better integration of the cells *in vivo* and ensures optimum room for vascularization of the construct as the encapsulating hydrogel degrades after implantation. Encapsulating cells at the macro (cm/mm or inch scale) and micron (less than  $500\mu\text{m}$ ) diameter spheres in different hydrogels like gelatin methacrylate (GelMA) and alginate have shown some success in the last decade in tissue engineering of liver, heart, cartilage, skin, and bone [5].





### 1.3 Importance of cell micro encapsulation:

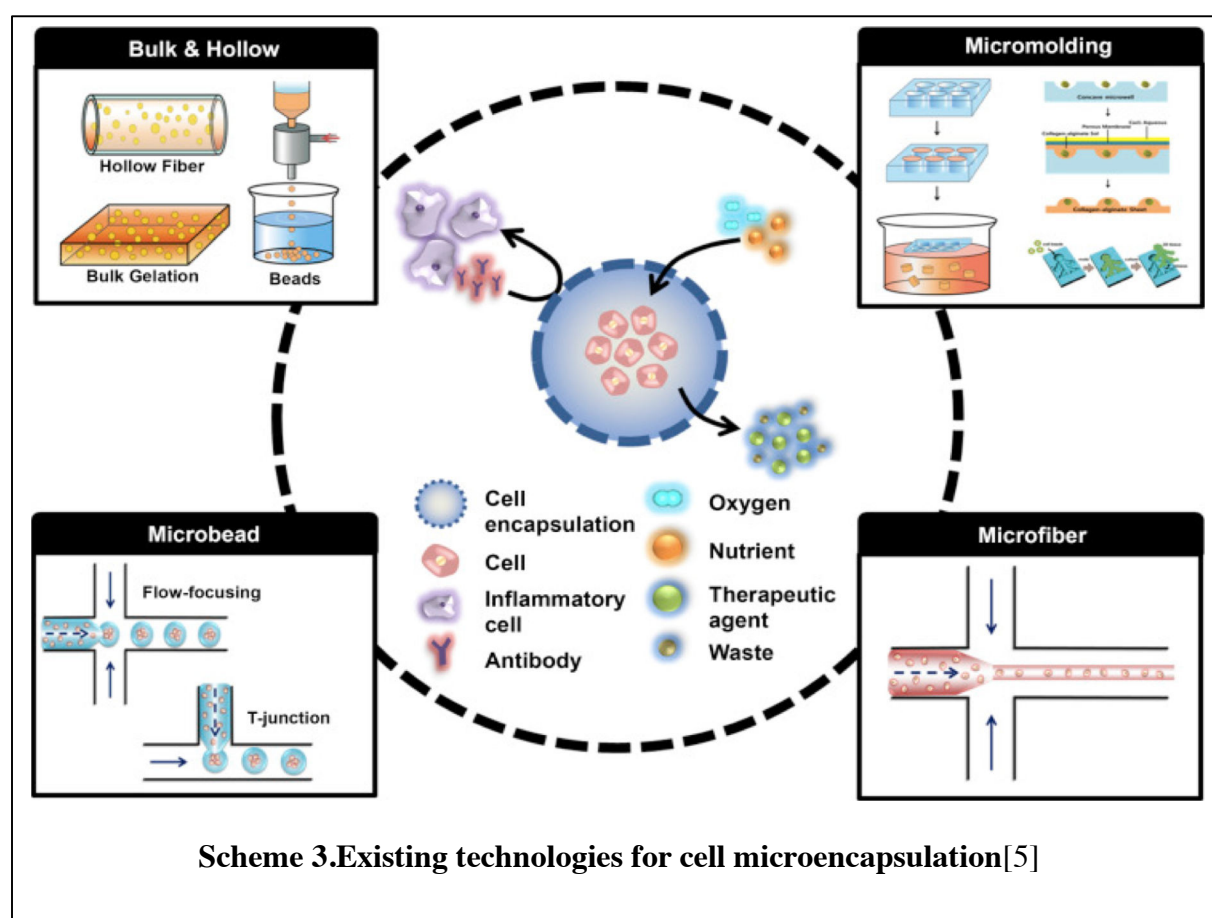
Cell encapsulation for tissue engineering therapy can be done both at the macro scale i.e. in spheres bigger than  $500\mu\text{m}$  in diameter and also at the micron scale i.e. in spheres smaller than  $500\mu\text{m}$  in diameter. Macro-encapsulation of cells in these hydrogels that mimic the *in vivo* environment to support the viability of cells serves as a good cell seeding strategy. However, scaffolds bigger than  $300\mu\text{m}$  in dimensions have issues of inadequate media and oxygen perfusion and inadequate vascularization leading to lower cell viability [6]. It has been demonstrated in the literature that it is essential to control the microsphere size to an optimal range to support maximum cell viability. It has been shown in the previous literature that for

microsphere sizes above 300 $\mu$ m a lower cell viability is generally observed [7]. Sawyer et al. suggested in their discussion that this could be due to the oxygen diffusion limit which inhibits cells from getting the necessary nutrition and causes low cell-viability [8]. A precise control over the size of these hydrogel microspheres plays a critical role in affecting the phenotypic characteristics like differentiation or induction or gene expression of the encapsulated cells making this a universal platform technology for stem cell therapy [8][9]. Microencapsulation of cells facilitates the even cell seeding since the hydrogels that encapsulate these cells in micro spherical emulsions themselves act as micron scale scaffolds. Due to the micron scale of these hydrogel microspheres, they are easily injectable thus potentially eliminating the need for highly invasive surgery required to implant larger scaffolds to treat 3D visceral tissue defects [10]. These micron scale structures can be made out of a variety of biocompatible hydrogels with varying concentration of prepolymer solutions and hence varying degradation rates [11]. This formed the basis of selecting a micro-encapsulation approach for potential applications in tissue engineering.

#### **1.4 Existing micro encapsulation techniques and their drawbacks**

Microfluidic devices have been extensively used for a wide variety of cell applications. The ability to study the effects of the microenvironment on cell growth, viability and differentiation with precision has made microfluidics their own industry with a predicted market value of billions of dollars [12]. The existing technologies have increasingly used micro encapsulation due to the small scale encapsulation of cells for a variety of applications in immunology, drug testing, determining the effects of a variety of biophysical parameters on cell-signaling, motility, survival, and differentiation [13]. The popular devices used for micro-scale encapsulation of cells

often require clean room fabrication techniques that are either complex or prohibitively expensive. Most of these techniques use microfluidic devices for cell encapsulation [14][15]. The current challenges facing the microfluidic devices used for cell encapsulation on the market are the complexity of fabrication and their dedication to encapsulate limited cell types [16][17]. Another issue associated with the microfluidic chips that are currently used for cell encapsulation is the lack of flexibility of the experimental set up with respect to efficiency of sample collection, microsphere size repeatability, and the number of cells per microsphere [8]. Scheme 3 shows the existing technologies for micro encapsulation used in laboratory research.



Bulk and hollow: In this approach, the cells are encapsulated in bulk hydrogel blocks or in hollow hydrogel fibers by pressurizing through a syringe nozzle or block casting of hydrogels. This is a macro-scale approach, however, can be used at a micron scale by 3D printing micron scale blocks of hydrogels laden with cells [5].

Micro molding: In these techniques, typically a master mold is fabricated using any lithography approach with the desired microstructures. The hydrogels laden with cells are pipetted into these microstructures, cross-linked and removed to yield the cell-laden microstructures [5].

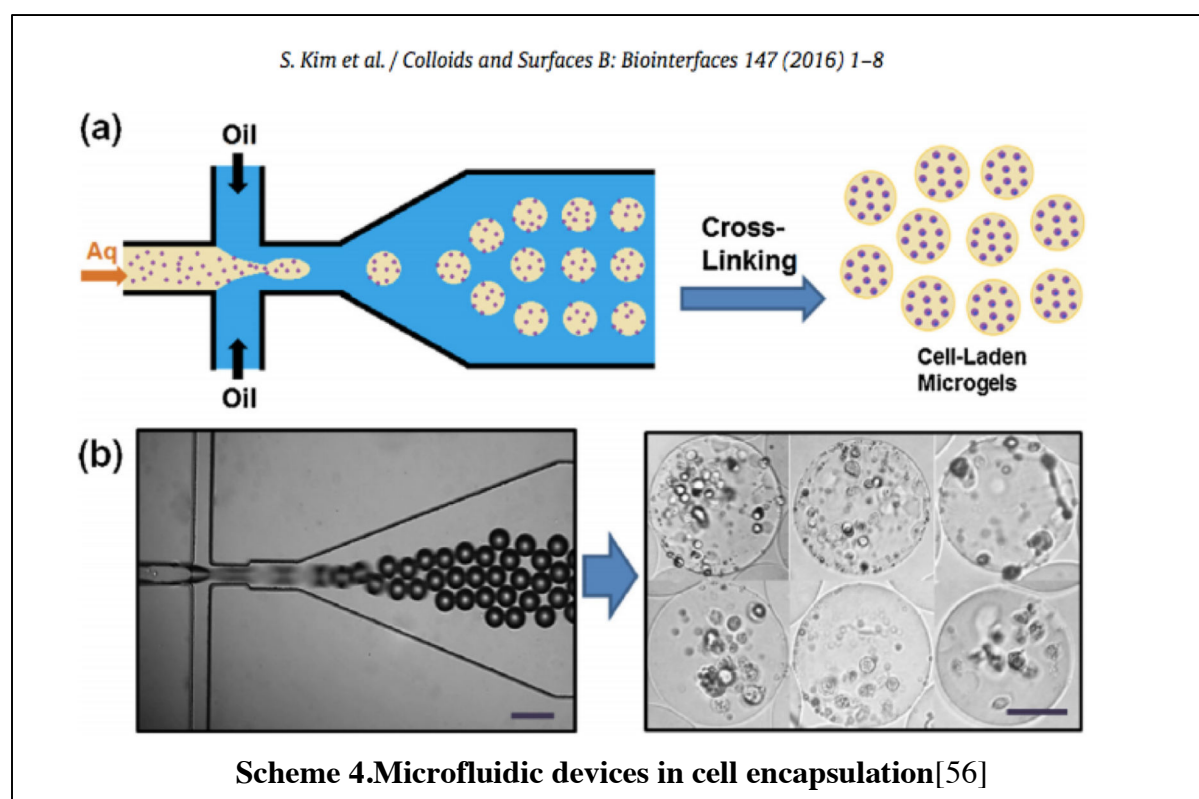
Micro bead/T junction: These are principally microfluidic devices that have two-micron scale channels that intersect in a T junction. The microencapsulation occurs at the T junction cross section[5].

Microfiber: This technique uses a capillary based microfluidic design to generate micron-scale diameter fibers of cell laden hydrogels [5].

Oil drop method is a technique of dropping cell-laden GelMA balls into an oil well so that the cell laden GelMA balls up into spheres coated with a layer of oil. Another group of widely used popular microfluidic devices for cell encapsulation employ the oil drop methods that use clean room fabrication approaches to create hydrogel emulsions which make them prohibitively expensive [18]. The oil drop techniques used currently do not allow a precise control of emulsion morphology or the number of cells encapsulated per sphere.

In this thesis work, a flow focusing T junction model is used. Flow focusing T-junction models are widely used in the synthesis of microspheres using a laminar flow of two immiscible phases [19][20]. A flow focusing T junction consists of two micron scale microfluidic channels that intersect at right angles to form a T shaped junction. One of the inlets is for an aqueous phase

which is usually the hydrogel laden prepolymer solution with cells. Scheme 3 shows the current flow focusing microfluidic devices and how they are used in cell encapsulation that allow encapsulating cells in micron scale spheres by controlling flow rates of the aqueous and the oil phases. The major concern with the existing T junction models was that the lipid phase or the oil phase used induced a very high shear stress on the hydrogel phase containing cells, which affect the cell viability that can be maintained [19][18]. For tissue engineering applications maintaining a high cell viability is of vital importance.



Regardless of the size of the resulting encapsulation constructs, the greatest limitation to the widespread use of microfluidic setups is their complexity of fabrication [21][22]. This is especially true for devices used for micron scale encapsulation of cells, which requires the use of traditional clean room fabrication techniques. Popular photolithography techniques using silicon

substrates have dimensional limitations and are restrictively expensive[23][16]. Fabrication techniques employ clean room fabrication approaches to create hydrogel emulsions which make them prohibitively expensive [2]. Even the oil drop techniques do not allow for a precise control of emulsion morphology or the number of cells encapsulated per sphere. Other fabrication approaches for microfluidic devices used for microencapsulation include silicon etching [24], mechanical micromachining [25], imprinting and hot embossing [26], x- ray photolithography, laser photo ablation [27], 3D soft lithography [28] and injection molding [29], all of which have very complicated and elaborate experimental set-ups [30]. In summary, a broad range of techniques have been used to make microfluidic devices that enable the formation of microspheres using hydrogel materials. Hydrogels have emerged as an ideal material for cell microencapsulation studies due to their resemblance to the native extracellular matrix [31]. However, factors such as the method of cross-linking, toxic concentrations of photo-initiators [32], porosity parameters and storage capabilities also influence cell viability under this approach [33]. Microfluidic devices for cell encapsulation using fluid flow focusing microfluidic devices have been used for numerous *in vitro* assays to study the viability and behavior of cells in micron scale scaffolds. These devices allow for a precise laminar flow of fluid phases with a wide range of viscosities, with the ability to manage their flow rates. Along with their dimensions on the micron scale, microfluidic setups may ensure emulsification of two distinct phases at the cross - section of the two channels, resulting in the creation of micro-spherical emulsion structures may serve as micro-scale scaffolds if the appropriate materials are used. The lack of precise control of encapsulation dimensions makes this process rigid and inflexible during translation into animal models for clinical studies. Efforts to improve these draw backs have led to numerous impetus on

developing fabrication techniques alternative to clean room approaches to fabricate microfluidic chips and molds.

**1.5 Goal of the thesis work:** The goal of this work was to engineer a universal microfluidic chip to enable the encapsulation of cells using a high resolution 3 D printing fabrication approach for the microfluidic mold to make the cell encapsulation process high throughput and ensure there is minimum process induced damage and sustained high cell viability.

## **Chapter 2: Experimental Design**

### **2.1 Methods and Materials**

This section elaborates on the hydrogel synthesis, device fabrication and cell culture protocols used in the experiments for both the non-cell and cell work.

#### **2.1.1 GelMA synthesis protocol**

10 grams of Type A Porcine gelatin were weighed and dissolved in 100ml PBS buffer in a three-prong flask immersed partially in a water bath. The water bath is set to heat a three-prong flask with magnetic stirrs both in, the bath and in the flask. The water bath is maintained at a temperature of 60-65°C. To remove the oxygen, rubber stoppers were used to block two out of the three outlets of the three-prong flask. One outlet was left uncovered to account for pressure buildup. One of the two rubber stoppers were punctured with a needle allowing argon gas to flow in at 10 PSI for 10 minutes to remove any oxygen introduced during the dissolution of the gelatin in the buffer. 8 ml of methacrylic anhydride was added very slowly using a 5 ml syringe needle through one of the rubber stoppers on the three-prong flask. The mixture is allowed to react for 3 hours. After 2 hours 45 minutes 100 ml PBS buffer was warmed up to 60°C for about 15 minutes to dilute the reaction mixture. 3.5 liters of millipore water was set aside in a large beaker on a hot plate to warm up to 70°C. A 12-14 kDa cellulose membrane was suspended in this millipore water bath allowing it to open up for about 10 minutes. One side of the membrane was clamped and the reaction mixture was poured into the cellulose membrane, clamped up on both sides and suspended in the millipore water for 1 week. The millipore water was changed every 12 hours for this one week. The reaction solution was then stored in centrifuge tubes and frozen overnight



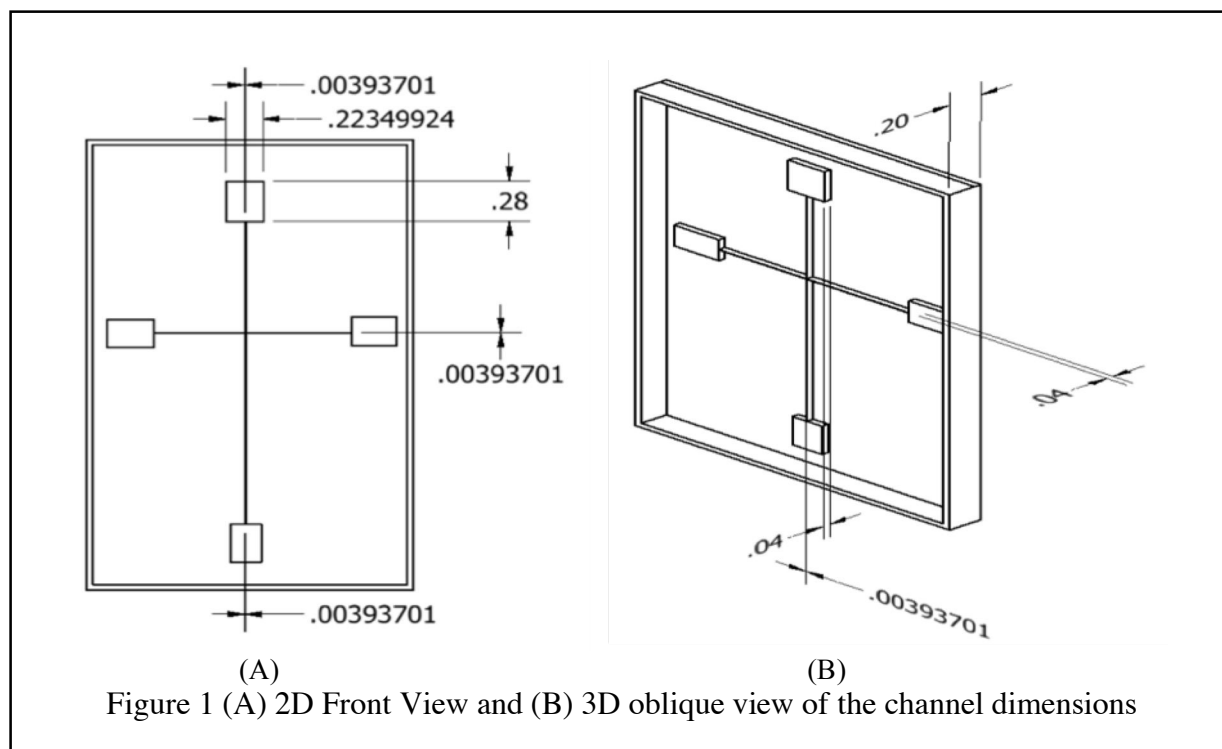
in a -80°C freezer. These tubes were then put in a lyophilizer and allowed to dry for one week. At the end of the second week, the GelMA was ready to use to make solutions of different concentrations. Irgacure 2959 was added to these solutions as a cross-linking photo initiator [34].

### **2.1.2 Device fabrication**

The device was designed on Inventor, a CAD design software. There are two channels intersecting at right angles to form a T junction. The channel width was defined at 150µm and the channel height at 2mm. The mold base was a rectangle 8mm in length, 5mm in width and 2mm in thickness. PDMS base and curing agent were hand-mixed well in the 4:1 ratio and degassed in a vacuum gasket for 30 minutes. The PDMS was poured on top of the mold and cured in an oven at 60°C for 3 hours to set it. After 3 hours, the PDMS was cut along the edge of the mold using an *xacto* knife and peeled out. The peeled portion of the PDMS was the negative of the mold, which was bonded face down to a glass slide using a plasma cleaner at Dr. Maroo's lab in Life Sciences Complex, Syracuse University.

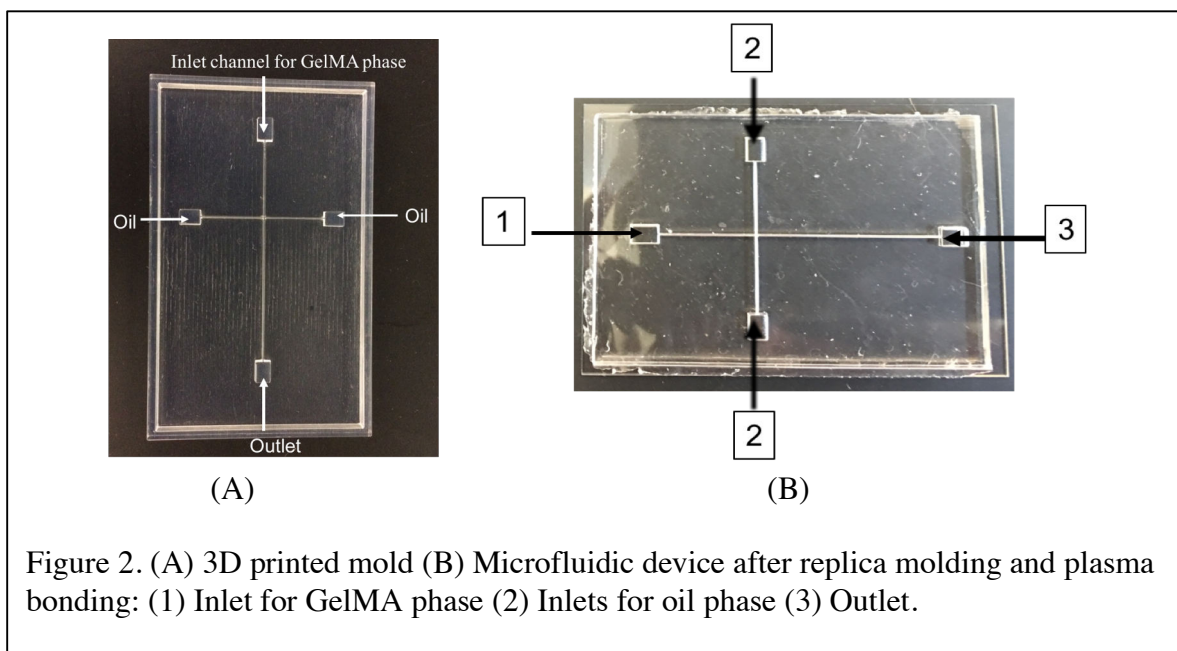
#### **2.1.2.1 Design and fabrication of the 3D printed microfluidic device**

The negative mold was designed for channel dimensions of 150 µm for both horizontal and vertical channel width, 4 mm channel height for all channels, the mold base was 4 mm thick and the mold rim was 5 mm in height. The inlet and outlet rectangular chambers were defined at 0.2234 inches x 0.28 inches (5.67436 mm x 7.112 mm). The chip was then connected to the inlets as shown in Figure 1.



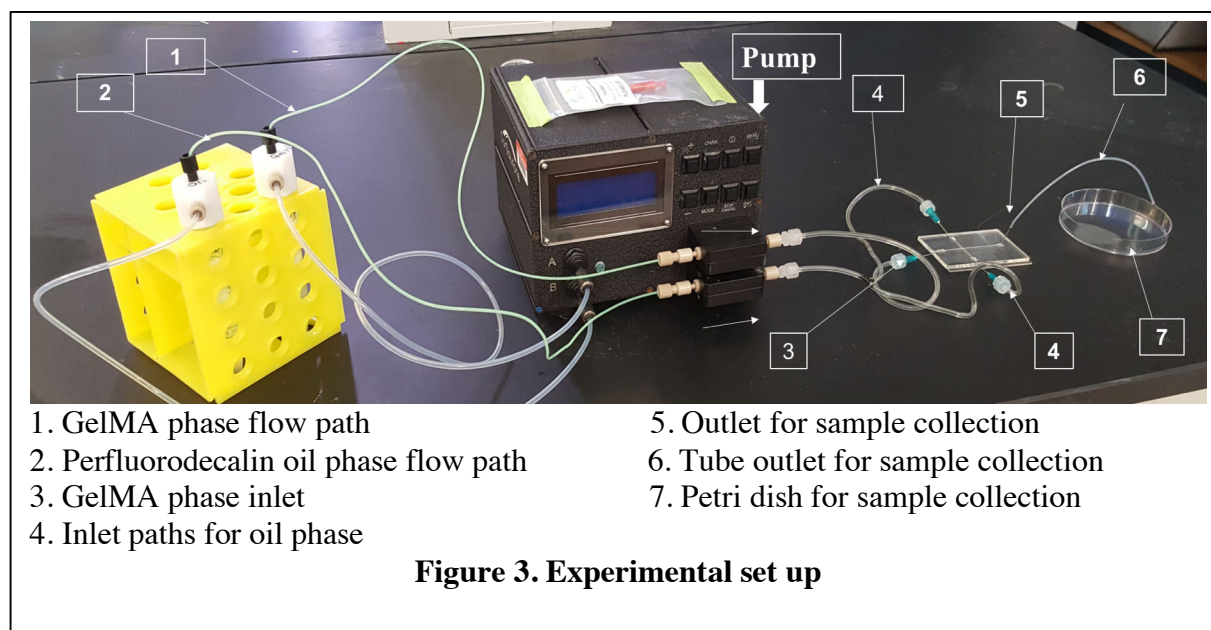
To fabricate the microfluidic chip the CAD design was extruded and exported as a .stl file to the Cornell NanoBiotechnology Center (NBTC) at Ithaca Cornell University, where it was 3D printed on a plastic like material called Vero-Clear using the ObJet 30 Pro 3D printer from Stratasys, Inc. This 3D printed showed a resolution of 16 microns for Vero Clear material (.0006 in.) [35] allowing us to 3D print fine channels with ease. This mold as shown in Figure 2 (A) was shipped back to our lab at Syracuse Biomaterials Institute, where it was cleaned by submergence in a solution of KOH 25% w/v solution in 15ml DI water and manual cleaning of the 3D printing left overs. This cleaning process was repeated three to four times to obtain a clean mold that was ready for Poly Dimethyl Siloxane (PDMS) casting. PDMS was mixed in the 1:4 ratio of curing agent to base, poured on the mold, vacuum degassed and cured in an oven at 60°C for 4 hours. Then this device was cut with a *xacto* knife along the edge of the mold and then peeled and plasma bonded to the glass slide as shown in figure 2(B) using the plasma cleaner facility. The

plasma radiation time of 1minute 30 seconds was used for each chip at an oxygen pressure of 10psi [36].



### 2.1.3 Set up:

The pump used to drive the encapsulation is the CorSolutions Pneu Wave dual channel pump. This pump operated on a pressure volume flow principle. The higher the pressure applied the higher the flow rate. The pump operates in a 0 -120  $\mu\text{l}$  /min flow rate range for pressures from 0-14.5 PSI. Figure 3 shows the entire experimental setup. The GelMA solution with and/or without cells flows through the tubing marked 1. The perfluorodecalin oil flows through the tubing marked 2 in figure 3. The GelMA phase enters the microfluidic chip at inlet marked 4 in figure 3. The oil phase enters the two inlets marked 3 in figure 3. The sample collection outlets are marked 5 on the figure. The samples (emulsions with microspheres) are collected through a tube marked 6 in figure 3. The samples are collected in a petri dish marked 7. These samples are then UV cross-linked.



## 2.2 Non-cell emulsion experiments:

To test the range of emulsions that could be achieved by this chip, solutions of different w/v concentrations of GelMA prepolymer were tested for their ability to form UV cross-linkable microspheres. 3%, 5%, 7%, 8%, 10% and 15% w/v GelMA prepolymer solutions were therefore made. The GelMA prepolymer solution flowed through the vertical channel as shown in Figure 2 (B) (Inlet 1) in the results section of this work, while the oil phase was a fluorinated oil perfluorodecalin, which has been found to successfully encapsulate hydrogels and assist osteogenesis in previous research [37]. The oil phase flows through the horizontal channels from both inlets as shown in Figure 2 B (inlet 2) in the results section of this thesis. The two phases merged at the cross section of the T junction in the chip where the microspheres are formed inside oil emulsions. These emulsions containing microspheres then flow out through the exit channel and are collected out of a needle from the exit channel. The volume of a single emulsion is typically 20  $\mu$ l that contains around 4510 microspheres. The emulsions were collected as subsequent squirts in a petri dish and irradiated with UV-light (Output power 850 mW, Omni

Cure S2000) for different exposure times corresponding to different concentrations of GelMA. To make the chip a universal platform for encapsulating all clinically relevant cell types, a threshold of the  $250 \times 250 \mu\text{m}^2$  cross sectional area was implemented. This resulted in microspheres ranging from  $30 \mu\text{m}$  to  $250 \mu\text{m}$  for different flow rate ratios and concentrations, the specifics of which are listed in the results section of this literature.

### *2.2.1 Viscometric characterization*

An AR-G2 Rheometer (TA Instruments, New Castle, DE) was used to obtain the viscosity at high shear of prepolymer solutions of varying GelMA concentrations. A parallel plate setup was used with a 40mm diameter steel geometry serving as the top plate. An implemental heating plate (522310.902 Peltier plate assembly) was used as the bottom plate to ensure the tests were performed at  $37^\circ\text{C}$  to replicate experiment conditions and prevent thermal gelation of the solutions. 2 ml of prepolymer solution was carefully pipetted at the center of the heating plate. A gap of 1.5 mm was maintained. The temperature was equilibrated for two minutes, after which the samples were subjected to a steady state flow procedure where the shear rate was ramped from  $0.1 - 1000 \text{ s}^{-1}$ .

### *2.2.2 Rheological Characterization*

An AR-G2 Rheometer (TA Instruments, New Castle, DE) with a parallel plate geometry (8 mm diameter) was used to determine the viscoelastic behavior of cross-linked hydrogel samples made from solution of different polymer concentrations.

$300 \mu\text{l}$  of each prepolymer solution was injected between two  $18 \times 18 \text{ mm}$  glass coverslips (Globe Scientific, Paramus, NJ) separated by a custom-printed PLA spacer with 1mm thickness.

Samples were then irradiated with UV for 60 seconds (Output power 850 mW, Omni Cure S2000). An 8 mm diameter biopsy punch (Robbins Instruments, Chatham, NJ) was used to cut out the hydrogel discs and detach them from the cover slips. The hydrogels were then incubated in ion-exchanged and distilled water at 37°C for 24 hr prior to characterization to remove any un-cross-linked gelatin prior to characterization. Rheological analysis was performed at room temperature using a gap size of 850  $\mu$ m. Frequency sweeps (0.1-100Hz) were performed at 1% strain to identify the behavior of the storage and loss moduli of the constructs. The intersection point between the two data trends was noted.

### *2.2.3 Injection experiment*

To test whether the obtained GelMA microspheres were stable when injected in and out of a syringe needle, 100 $\mu$ m and 150 $\mu$ m sphere sizes were tested. The pressure was scaled to obtain flow rates of 62.5 $\mu$ l/min for GelMA phase and 89.32 $\mu$ l/min to obtain an average sphere size of 100 $\mu$ m repeatedly with good consistency. The flow rates of 72 $\mu$ l/min and 95.26 $\mu$ l/min were used to yield an average sphere size of 150 $\mu$ m with good consistency; both for 8% GelMA concentration in 13mL of PBS buffer. These samples were UV cross-linked (output power 850 mW, Omni Cure S2000) for 90 seconds and suspended in DI water. A bright field image was taken before these spheres were sucked into the 23-gauge needle with a mean diameter of 641.35 $\mu$ m. Then another image was taken after these spheres were injected out of the needle, after which these spheres were suspended in 20 $\mu$ l of DI water.

## **2.3 Cell Experiments:**

### **2.3.1 Step 1: Component sterilization: Autoclaving**

To ensure that the encapsulation occurs in a perfectly sterile environment we autoclaved all the tubing that came in any contact with the cell solution. The fittings and connectors like the luer locks, Y- junctions and inlet and outlet hoops were soaked in 100% cell culture grade ethanol in a biosafety hood under UV light to sterilize, as autoclaving damages them due to their lower temperature thresholds. The microfluidic chip was autoclaved as well to prevent any bacterial contamination of the GelMA emulsions within the chip. The autoclaving temperature was set at 120°C, where the tubing was autoclaved for a 30-minute cycle and the oil autoclaved for another 30/30 cycle. Autoclaving the tubing, devices and the oil is essential to ensure there is no bacterial contamination [38].

### **2.3.2 Step 2: Making GelMA prepolymer solution**

To make GelMA prepolymer solutions, a desired volume of buffer is filled in a centrifuge tube. For most of the experiments 13 mL of buffer were used to make the prepolymer solution. An appropriate amount (desired w/v concentration) of frozen GelMA polymer was weighed and dissolved in the buffer. To enable crosslinking 0.25% Irgacure 2959 photo initiator was added. This weight/volume ratio of 0.0025 was critical and has been found to work for previous research groups [2]. The centrifuge tube was then stored in an incubator at 37°C and left overnight to ensure that the GelMA dissolved completely and was adequately degassed before being sterile filtered.

### **2.3.3 Step 3: Making the Cell solution**

The GelMA prepolymer solution was sterile filtered using a non-pyrogenic Corning Incorporated 28 mm micron membrane syringe filter (28 mm 0,20 SFCA) into a sterile centrifuge tube to ensure there is no bacterial or process induced contamination in the GelMA prepolymer solution. The vile containing the suspended cells is removed from the incubator and the old media is aspirated. The cells are then trypsinised.

#### 2.3.3.1 Cell Solution protocol

Take 250 mL Saos-2 cell flask out of incubator. Under hood, use vacuum to remove DMEM (Dulbecco's Modified Eagle's Medium) media from the flask. Fill the flask with 10 mL of PBS (Phosphate Buffered Saline) to remove excess media. Vacuum out PBS. Add 5 mL of trypsin. Place flask back in incubator for 5 minutes. Remove flask after 5 minutes and tap the sides of the flask to detach the remaining cells from the bottom of the flask and into the trypsin solution. Add 15 mL of media to the flask to counteract the trypsin. Mix well, and transfer the trypsin/media/cell solution into a 50 mL tube (should have 20 mL of solution). Take 10  $\mu$ L of the solution and place it in one well of a 64 well plate. In the same well add 10  $\mu$ L of Trypan blue dye. Mix and place 10  $\mu$ L of the dye solution under the glass slide on the Hemocytometer. Take the 50mL tube and place it in the centrifuge across from a 50 mL tube filled with 20 mL DI water (for balance). Centrifuge at 200 rpm for 10 minutes. While centrifuge is running, count cells using 40x microscope and a clicker (ex. Yield 10 million cells). Also, while centrifuge is running, sterile filter 13 mL of GelMA (you will most likely get 11 mL post sterile filter) into a



15mL tube. Set GelMA aside. Retrieve 50 mL tube with solution in it from centrifuge and vacuum the media out (you should see the cells congregated at the bottom.) Add of media to the 50mL tube with just the cells in it and mix (ex. this will give you 10 million cells per 1 mL of media.) Transfer this 1 mL of cells/media into the 15 mL GelMA tube and mix well [2].

#### 2.3.3.2 Osteosarcoma Cell culture

Human osteosarcoma cells (Saos-2; ATCC) were used for cellular encapsulation studies[2].

Saos-2 cells were cultured in Dulbecco's Modified Eagle's Media (DMEM; Life Technologies) supplemented with 1% penicillin-streptomycin (PS, Life Technologies), 1% GlutaMAX (G, Life Technologies), and 10% fetal bovine serum (FBS lot G12102, Atlanta Biologicals), within a humidified 37°C incubator containing 5% CO<sub>2</sub> [2]. Prior to encapsulation, cells were grown to confluence and passaged using 0.25% trypsin-EDTA (Life Technologies). Cells were encapsulated in GelMA by mixing 1 mL of a cell solution density of approximately 6 million cells with 10 mL of 8% (w/v) GelMA solution[2]. The GelMA/cell solution was mixed thoroughly prior to encapsulation and was kept warm throughout the process. After encapsulation, oil emulsions containing GelMA microspheres were transferred into cell culture media. Media was changed on the emulsions every 2 to 3 days using standard cell culture procedures[2].

#### **2.3.4 Step 4: The encapsulation process**

The solution contain suspended Saos-2 cells in GelMA prepolymer solution was flowed through the vertical channel of my chip. The oil phase consists of a fluorinated oil perfluorodecalin[37] that is found to assist bone regeneration as well as found success in previous encapsulation

studies. The oil phase flows through both inlets of the horizontal channel. The two fluid phases intersect at the T junction where there is formation of the emulsion spheres. The cross-sectional area of the T junction is  $150 \times 150 \mu\text{m}^2$ . This size allows creation of stable emulsion spheres ranging from 20 to 250  $\mu\text{m}$  in diameter. This allows immense flexibility in the number of cells that we can encapsulate in each emulsion sphere. These emulsions flow out through the vertical exit channels where they flow out through a needle inserted in the exit channel. These emulsions were collected in petri dishes and then UV cross-linked for exposure times varying according to the concentration of GelMA in each solution. The UV crosslinking times observed for 5%, 7%, 8%, 10% and 15% w/v solutions were all under 120 seconds which is conducive for crosslinking GelMA without killing cells encapsulated within. These encapsulated cross-linked samples were then transferred to a 24-well plate in the biosafety hood. They are then stored in 1mL complete DMEM media in the incubator to ensure cell viability before staining.

### **2.3.5 Staining:**

#### **2.3.5.1 Live/ dead staining:**

Live/Dead staining and image processing:

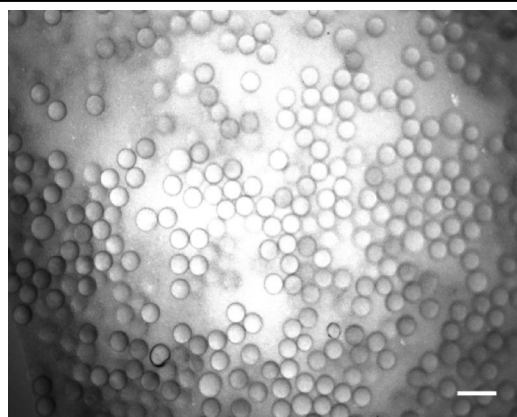
The viability of cells was determined using a Live/Dead assay. In order to determine cell viability, emulsions containing cell-laden spheres were submerged in media containing Calcein-AM (1:2000 dilution; Corning) and ethidium homodimer (1:500 dilution; Life Technologies), and incubated at 37°C for 1 hour prior to imaging [2]. Emulsions were analyzed at 1 day, 1 week, 2 week, and 3 week time points, respectively.

Raw .tiff fluorescent images were taken of the stained emulsions using a Leica DMI4000 B inverted microscope (Leica Microsystems GmbH), and were analyzed using open-source ImageJ (NIH) software. The images were tuned for brightness and contrast.

## Chapter 3: Results and Discussion

### 3.1 Non-cell GelMA microsphere synthesis:

Figure 4 (A) shows the microspheres obtained for flow rates of 35  $\mu\text{l}/\text{min}$  for GelMA phase and 50  $\mu\text{l}/\text{min}$  for oil phase which generated microspheres of  $\sim 33$  to 35  $\mu\text{m}$ . The UV cross-linking time observed for different concentrations of GelMA solutions was recorded and reported in Figure 4 (B) Table 1. Through experiments, it was observed that it is possible to fabricate GelMA microspheres with an optimal UV cross-linking time and viscosity efficiently and with maximum repeatability for 5 to 15% w/v GelMA concentrations. It was observed that for less than 5% GelMA concentration, the UV cross-linking time required is over 3 minutes which would be lethal for encapsulating cells in these microspheres and it is also very difficult to crosslink lower than 5% w/v concentrations of GelMA.



(A)

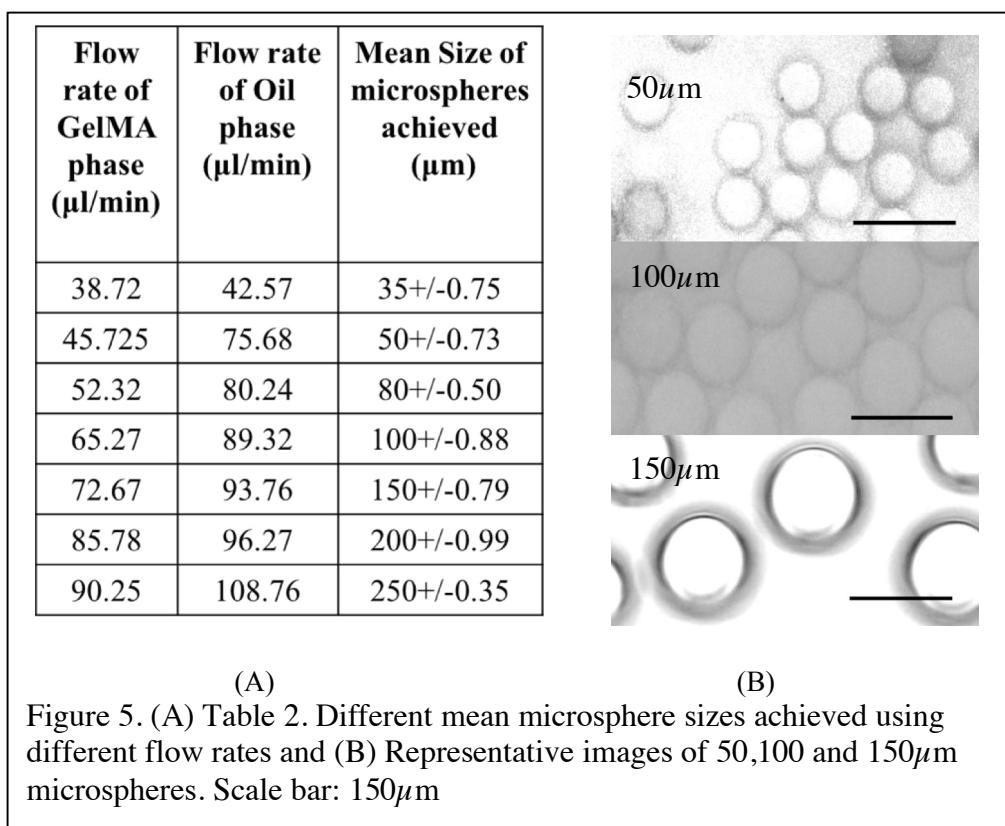
GelMa Concentration (%)	UV Crosslinking time (sec)
5	250
7	170
8	115
9	90
10	60
15	45

(B)

Figure 4. (A) GelMA microspheres 35 $\mu\text{m}$  in mean diameter made from 8% (w/v) GelMA (Scale bar: 50  $\mu\text{m}$ ) and (B) Table 1. Representing UV crosslinking time for crosslinking microspheres made from different (w/v) concentrations of GelMA.

Different flow rate ratios of the GelMA phase and the oil phase yield microspheres of different mean sphere sizes. With this microfluidic chip, it was possible to create microspheres 35 to 250

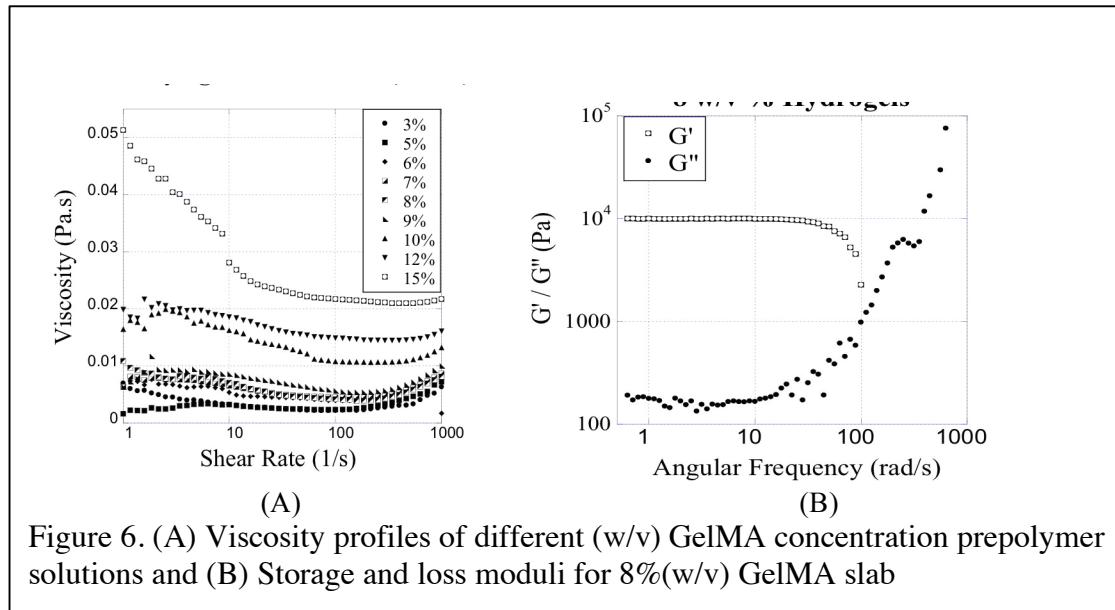
$\mu\text{m}$  in diameter with maximum repeatability. Table 1. shows the different flow rates used for the GelMA phase and oil phase to obtain different sizes of microspheres. The standard deviation values are low indicating a high degree of uniformity achieved in the obtained microspheres. The results of this experiment indicate the range of GelMA concentrations that is optimal to effectively make injectable hydrogel microspheres to serve as scaffolds of micro scale that can potentially encapsulate all clinically relevant cell types. Figure 5 (A) Table 1 represents the average size of GelMA microspheres achieved with 8% (w/v) GelMA solution at varying flow rates. Each solution concentration flowed at three distinct flow rate ranges and it was observed that varying these values resulted in microspheres of distinct sizes. As an example, the following trends were observed for the 8% (w/v) GelMA phase and the standard oil phase respectively. For flow rates of 45.725  $\mu\text{l}/\text{min}$  for GelMA phase and 75.68  $\mu\text{l}/\text{min}$  for oil phase (8% w/v GelMA concentration), repeated microsphere mean size  $\sim 50 \mu\text{m}$ -corresponding to these flow rates. For flow rates of 65.27  $\mu\text{l}/\text{min}$  for GelMA phase and 89.32  $\mu\text{l}/\text{min}$  for oil phase (8% w/v GelMA concentration) repeated microsphere mean size  $\sim 100 \mu\text{m}$  corresponding to flow rates. For flow rates of 72.67  $\mu\text{l}/\text{min}$  for GelMA phase and 93.76  $\mu\text{l}/\text{min}$  for oil phase (8% w/v GelMA concentration) repeated microsphere mean size  $\sim 150 \mu\text{m}$ -corresponding to the flow rates. After repeating these trials, these values were found to be consistent.



### 3.2 Characterization of material properties:

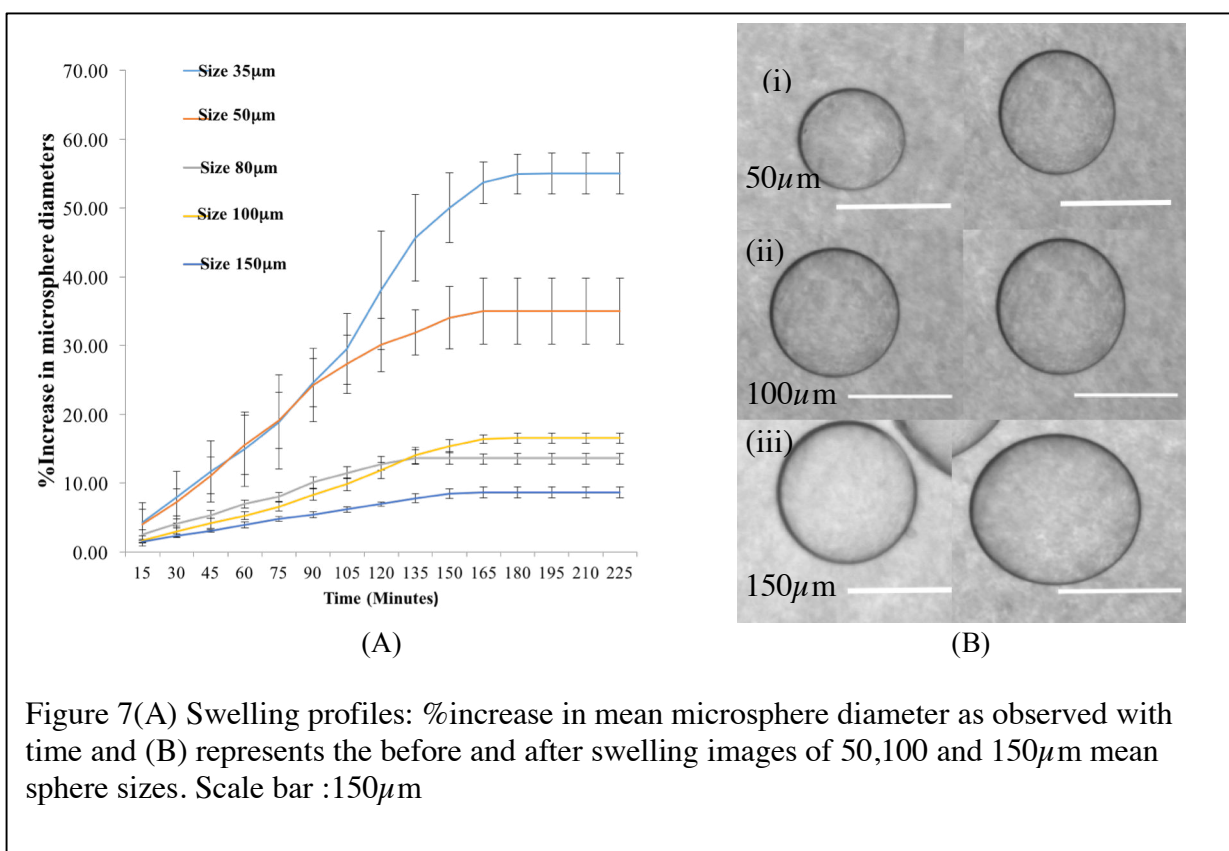
The hydrogel used for cell microencapsulation in this work was tested for different w/v prepolymer solution concentrations. The viscous and rheological properties of these prepolymer solutions were characterized. Figure 6 (A) represents the viscosity profiles of different (w/v) GelMA prepolymer solution concentrations. The viscosity varies as the shear rate on the parallel plate is varied from 1 to 1000  $\text{s}^{-1}$ . Non-cell experiment work was necessary to optimize conditions and characterize our materials. Physical characterization was centered on observing the hydrogel storage and loss moduli for different concentrations of GelMA. Figure 6 (B) represents the storage and loss modulus of an 8% (w/v) cross-linked hydrogel disc. This was done to approximate the stiffness of the matrix environment experienced by the cells once in

their encapsulated form. Solution viscosity was a focal point of study [39] to identify the maximum concentration that could be used that would optimally flow through the setup at the high flow rates to be used, especially since the laminar flow was required to effectively form our microspheres. The temperature and the flow rates corresponding to this shear rate were determined to be the thresholds (minimum flow rate) required to form emulsions at these solution concentrations. To quantify the mechanical nature of microspheres made out of these pre-polymer solution concentrations, rheological characterization of the loss and compression modulus was done [40]. A comparison of the viscous and mechanical properties of varying w/v concentrations of GelMA helped us determine the w/v concentration range and narrow down on the GelMA concentrations that work best for cell encapsulation experiments that are discussed in the following section.



Microspheres of specific dimensions were expected to show unique swelling behavior which is shown in Figure 7. Figures 7(i - iii) represent the swelling observed for 3 repeatedly achieved microsphere sizes using 8% (w/v) GelMA. It was observed that the microsphere with 50 $\mu$ m

initial mean diameter saw a 35.01% increase in diameter. Samples with a 100 $\mu\text{m}$  initial mean diameter saw a 16.54% increase in diameter, while the larger microspheres with a mean diameter of 150  $\mu\text{m}$  initial mean diameter also saw a small increase in diameter but only of about 8.6% after complete swelling. For all tested samples, it was observed that the completely swelled state was reached after about 2 hours 30 minutes, after which no significant change in dimensions was observed. The stepwise mean %increase and standard deviations are listed in a table in the Appendix A Section C of this work.





The overall range of microsphere diameter achievable with this microfluidic chip using this two-variable experimental set up was  $\sim 30$  to  $250\ \mu\text{m}$ . Figure 8 represents the before and after injection images for a  $20\ \mu\text{l}$  emulsion volume of  $100\ \mu\text{m}$  mean sphere size. There was no disruption of the microsphere size observed upon injection in and out through a 20-gauge needle. There was some disruption in microsphere shape observed upon injection through a 23-gauge needle for a mean microsphere size of  $100\ \mu\text{m}$ .

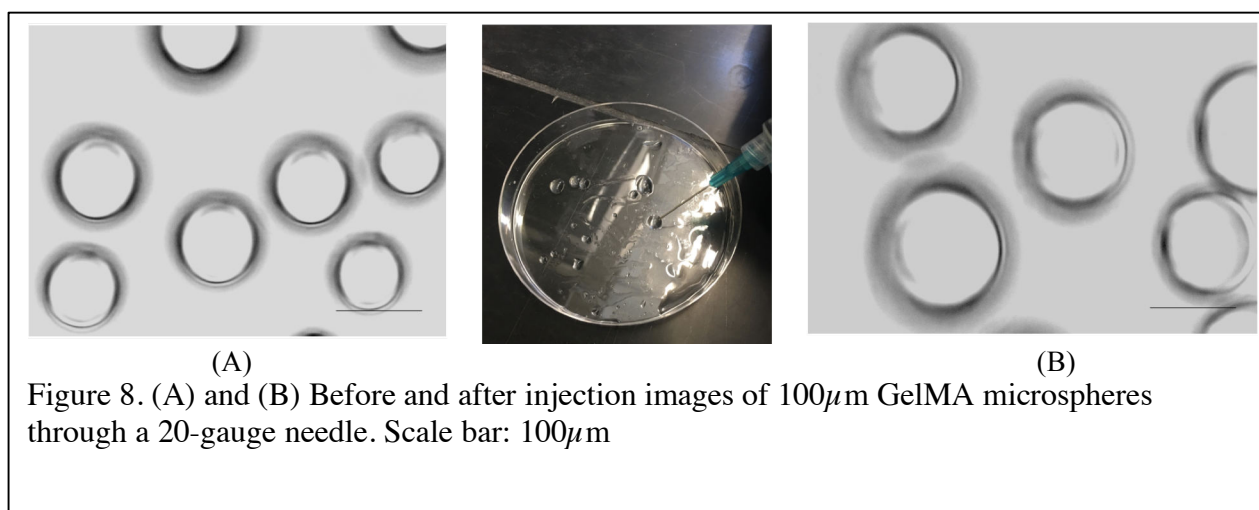
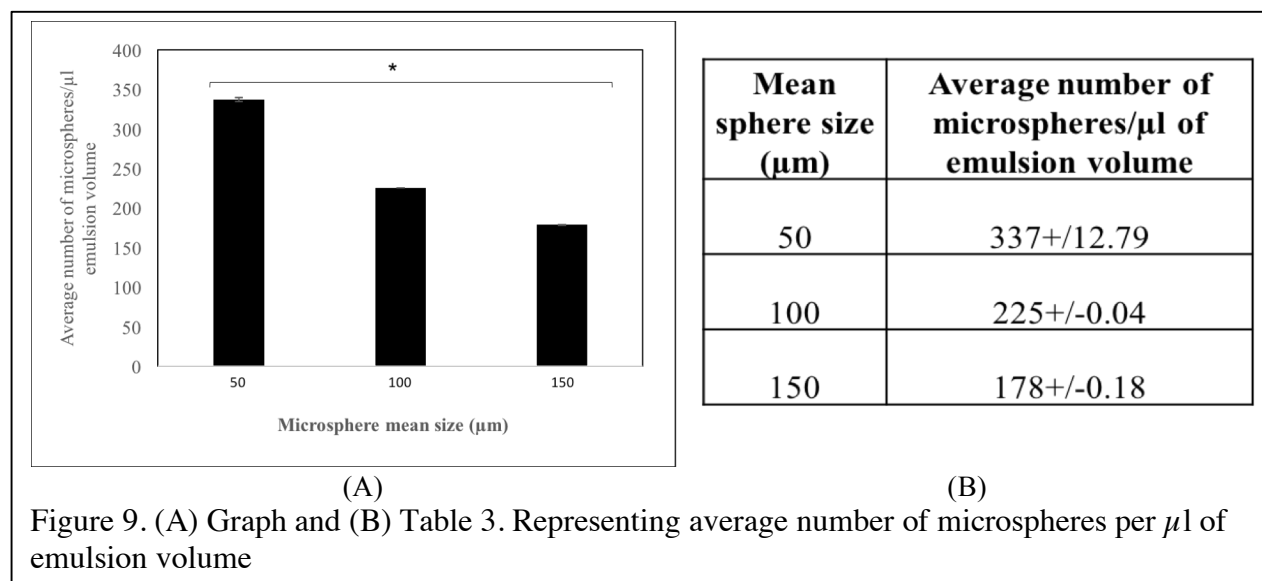


Figure 9 represents the average number of microspheres of  $50, 100$  and  $150\ \mu\text{m}$  mean sphere size per  $\mu\text{l}$  of emulsion volume. The microspheres are laden in an oil emulsions which were ejected as  $20\ \mu\text{l}$  emulsions from the outlet of the microfluidic chip. This table and graph give an estimate of the number of microspheres obtained per unit volume of an emulsion.



### 3.3 Cell Encapsulation experiments

A solution concentration of 8% (w/v) GelMA was selected for all cell encapsulation work based on all these studies. The viscosity of this prepolymer solution was shown to exhibit laminar flow through the pump setup when at 37°C most efficiently, which is the required temperature to maintain cell viability. The UV exposure time required to cross-link the resulting microspheres was also low enough to ensure that this viability was maintained. The constructs also exhibited structural stability when incubated for three weeks. Figure 10 (A) shows a single emulsion sphere 100  $\mu\text{m}$  in diameter with cells encapsulated within. The image was taken after performing the cell encapsulation experiment when the microsphere was in media. The image is taken at 40x bright field using an inverted microscope. It was observed that larger microspheres encapsulated a greater number of cells. Figure 8 (A) and (B) shows ~28 cells encapsulated in a 100  $\mu\text{m}$  sphere in media and oil respectively.

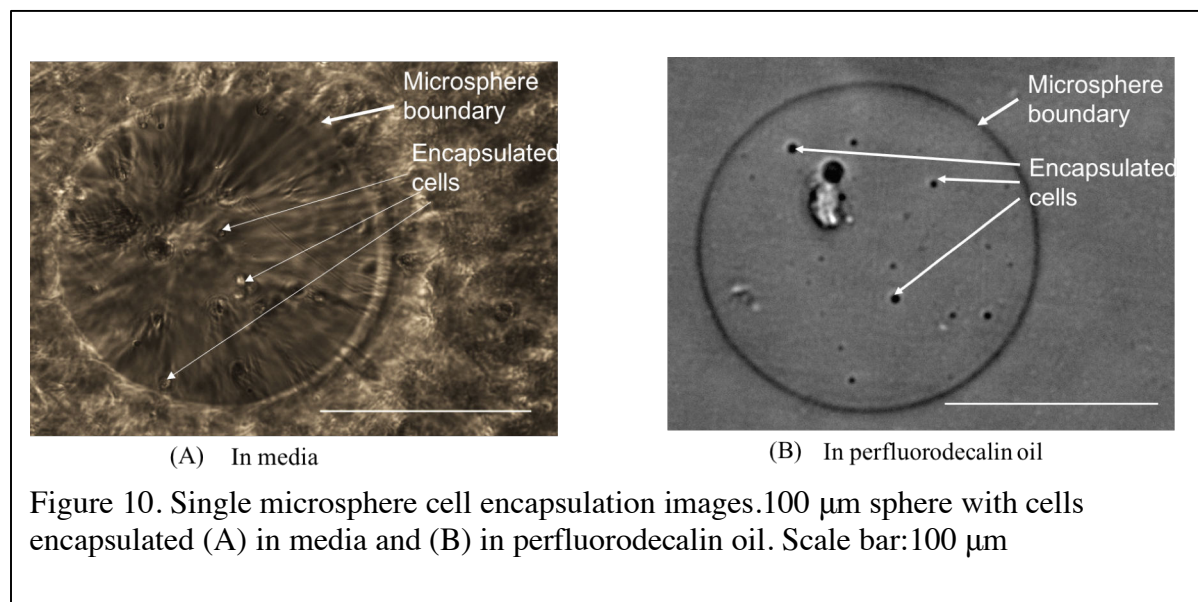


Figure 11. (A) Represents the number of cells encapsulated in spheres of different sizes. The number of cells that can be encapsulated increases with an increase in the size of the microsphere. The 100  $\mu\text{m}$  sphere as shown in Figure 11 (A) has around 28 cells encapsulated within. The cell concentration plays a key role in determining the cell encapsulation density per microsphere. The cell density that proved most effective was  $6 \times 10^6$  cells per 1 ml cell media added to 11 ml i.e. 545,454 cells/ml GelMA prepolymer solution after sterile filtering. Different cell densities dictate how much volume of each microsphere is occupied. This also largely depends on the cell dimensions or the shear rate used. In this setup, we used Saos-2 cells which are approximately 8-10  $\mu\text{m}$  in diameter [41]. Through our experiments, we identified that for cell densities greater than 545,454 cells per ml cause excess shear stress on the cells when they flow through the tubing that leads up to the device inlet. Figures 11 (A) and (B) represent the number of cells encapsulated per microsphere of different mean microsphere diameters. It is evident from the graph that as the mean microsphere diameter increases, the number of cells encapsulated per

microsphere increase. A test of significance for correlation coefficient was performed on this data and it was found that there is a significant correlation between the microsphere mean diameter and the number of cells encapsulated.

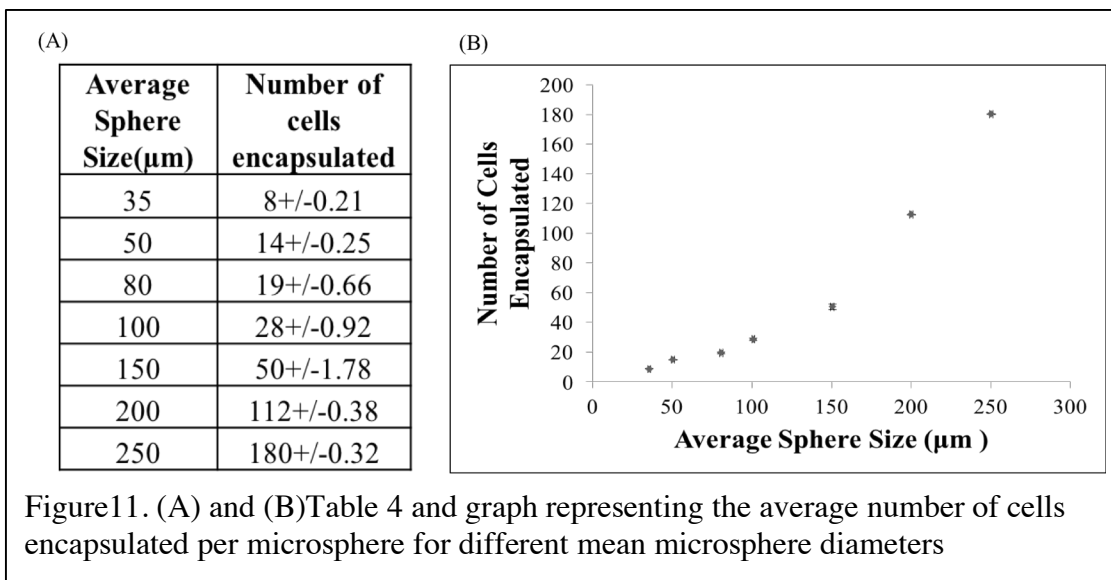
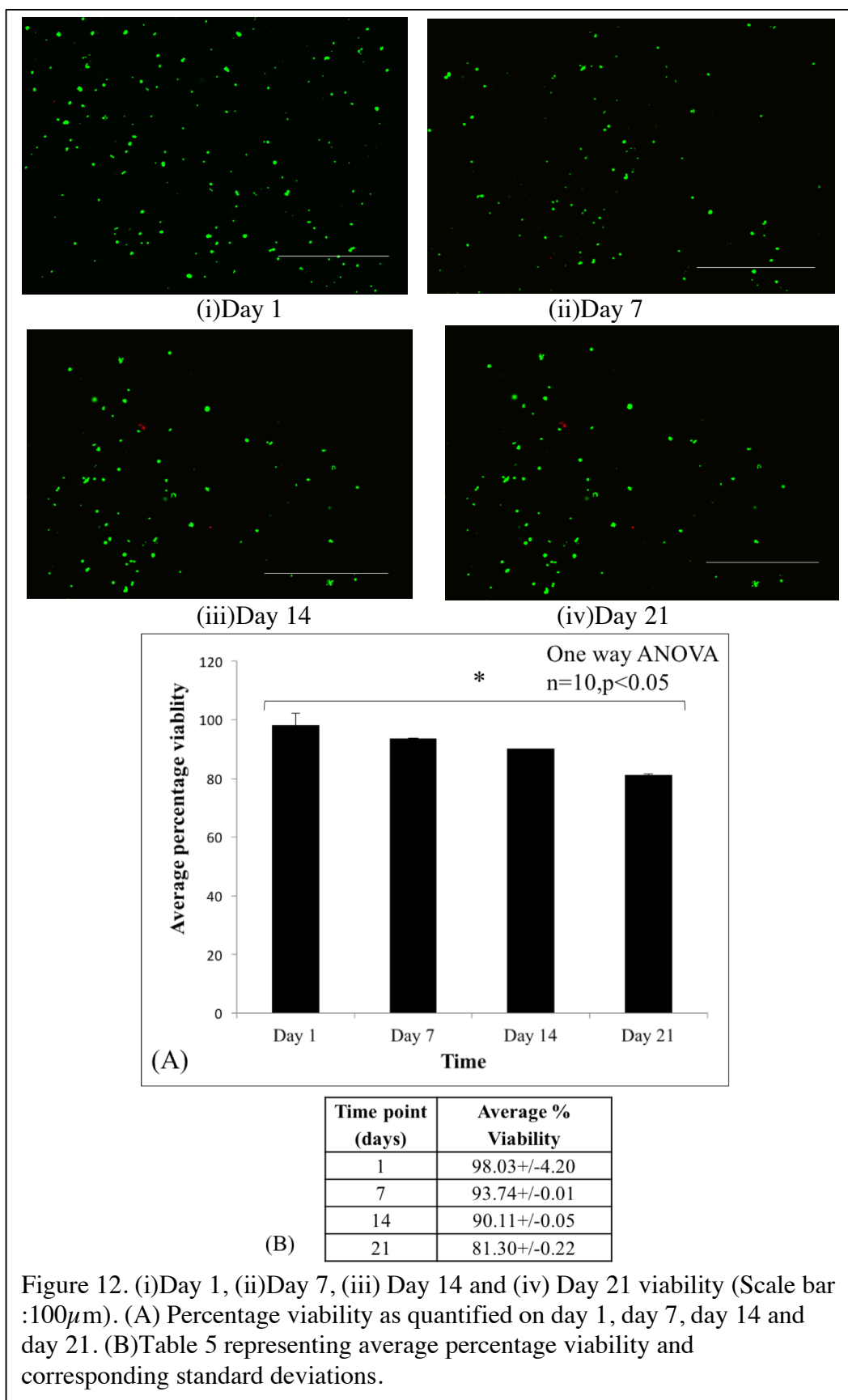


Figure 12 represents the %Viability of cells as observed for 100  $\mu\text{m}$  spheres on Day 1, Day 7, Day 14 and Day 21. We observed a cell viability of 98.03% on Day 1 indicating that this process is fairly mechanically robust and biocompatible enough to not introduce a significant process induced damage or contamination. A viability of 93.75% on Day 7, 90.125% on Day 14 and 81.25% on Day 21 was observed. The Figures 12 (i), (ii) and (iii) show the actual live /dead staining progression from Day 7 through Day 14 to Day 21. An ANOVA analysis was performed on this viability data which is listed in the Appendix A Section D section of this thesis, which reaffirms the visually obvious significant difference in the cell viability over the three week incubation period. Cell density plays a key role in determining the cell encapsulation density per microsphere. The cell density that proved most effective for our trials was  $6 \times 10^6$  cells/mL of cell

media added to 10mL GelMA prepolymer solution (11mL total). Different cell densities dictated how much volume of each microsphere was occupied. Limited process-induced damage was observed as cell viability remained close to 100% immediately following the procedure. Incubation over a three-week period showed that viability only decreased by ~20%. This shows that our encapsulated cell samples may be stored without the need for cryopreservation. Cell density was also shown to play a role in influencing cell viability. Densities higher than the 6 million cell count was shown to cause a decrease in cell viability when encapsulated. Additional factors such as cell size and applied shear stress resulting from an increased cell density during the encapsulation procedure would be expected to play a role in cell viability when using other cell types. We can therefore assume that use of larger cell strains may exhibit a different viability profile as oppose the Saos-2 cell quantified for this work, and therefore we may need to optimize an appropriate cell density to achieve the similar viability statistics.



Cell viability depends on the coordination between multiple parameters. The GelMA concentration used, the cell density used, the viscosity of the solution, and the temperature of the experimental set up. These were identified by experimenting with multiple GelMA concentrations, cell densities starting from 10 million cells and decreasing and adjusting the temperature and distance of the heating fan used to maintain the temperature of 37 °C. Also, it is essential to ensure that all the tubing, connection, devices and collection petri dishes are either autoclaved or sterilized by soaking them in 100% fill line ethanol to make sure that there is no contamination or process induced damage to the cells.

## **Chapter 4: Discussion, conclusion and future scope**

### **4.1 Discussion**

This section represents a comparison of existing cell micro encapsulation approaches and the improvement over the existing techniques in the aspects of fabrication approach, cell viability, high sample collection efficiency, high microsphere size repeatability and uniform number of cells laden per microsphere. The results presented in this work have shown a significant improvement over certain impediments to the existing cell micro encapsulation approaches over factors of (i) fabrication approach, (ii) cell viability, (iii) high sample collection efficiency, (iv) high microsphere size repeatability and (v) uniform number of cells laden per microsphere. The mold used to cast the microfluidic devices was fabricated using a 3D printing fabrication approach and PDMS casting and molding technique.

### **4.2 Research approach**

The novelty of this design allows immense flexibility of the size of microspheres that can be made and used to encapsulate a varying number of cells per microsphere depending on the cell density used in your cell solution and the size of microspheres. Due to the small size of achieved microspheres, they are injectable and hence can potentially help eliminate the need for surgery [42]. This engineered chip enables micron scale encapsulation of all clinically relevant cell types in emulsion spheres ranging 30 to 250  $\mu\text{m}$  in size. Due to the small size and range of encapsulation, effective media and oxygen diffusion is possible, thereby showing enhanced cell viability as demonstrated in my results. The flexibility in choosing varying concentrations of GelMA to encapsulate cells allows control on properties like swelling and degradation of the



hydrogel microspheres. Also, there is control of parameters like viscosity and mechanical robustness of the used hydrogel concentrations. To support and hold the cells in place it is essential that they are seeded inside a support structure or a scaffold. Many times, cells do not get evenly seeded in the scaffold. The microspheres generated by this chip allow the creation of cell laden microsphere scaffolds which ensure adequate and even cell seeding all throughout the size of the injury or defect which needs the tissue engineered construct [43]. Due to their small size, these microspheres can be injected at the site of tissue injury without the need for imminent surgery. This exciting hypothesis is what has led to the application of microencapsulation approach for this work.

This approach of micron scale encapsulation in hydrogel makes it a lot easier to preserve these micro-scale scaffolds in a normal well plate in an incubator instead of cryopreserving the construct. Cell viability is determined by a variety of parameters: toxicity and the amount of photo initiator [44], the degradation rate of encapsulating hydrogel, cell media and oxygen perfusion, porosity and interconnectivity of the scaffold, cryopreservation, storage requirements and the duration of storage [33][45]. The system designed in this work proposes a highly flexible and customizable technique to create hydrogel droplet scaffolds that resize all such parameters to help achieve enhanced cell viability. The PDMS based closed chip is made out of a 3D printing [46] and replica molding [47] approach which ramps up the ease of fabrication to your lab bench. Being an inexpensive polymer, you can make a large number of these chips and use them for encapsulation applications of various kinds of studies. This work presents an inexpensive microfluidic chip fabricated through 3D printing [48] followed by a replica casting and molding

technique [49]. The system designed proposes a highly customizable technique to create hydrogel droplet scaffolds that resize all parameters to help achieve enhanced cell viability.

#### **4.2.1 Fabrication approach:**

Popularly used microfluidic devices are manufactured using micromachining approaches with glass or silicon substrates. These micromachining approaches involve processes like chemical etching, lithography approaches that require a clean room for cleaning processes. Laser ablation approaches that need the use of high intensity laser beams to micro machine channels in different substrates. Other techniques like hot embossing, injection molding require thermoplastic substrates that have heat expansion related dimensional changes in the channels which impact the generated microsphere sizes and uniformity which varies with temperature [50]. In this work, the negative to the closed PDMS chip is made using a traditional 3D extrusion printing [51] and replica molding approach, which ramps up the ease of fabrication of multiple devices. In using Vero-clear plastic [52], an inexpensive polymer, multiple chips designs can be made on a budget and used for encapsulation applications for a wide variety of studies. It should be noted that for objectpro30 3d printer model RGD525, RGD430 and RGD450 [53] polymers can also be used in the printing process [35]. The use of PDMS as a casting agent facilitates the manufacture of multiple devices from a single print. After a careful deliberation of choice of 3D printing polymer and vertical resolution and ease of use and access, we decided to go ahead with the Stratasys Objet Pro30 model desktop size 3D printed to fabricate the microfluidic device used for microencapsulation in this work. The use of GelMA over synthetic hydrogels like PEG-DA has significantly increased over the past decade in cell microencapsulation applications [54] [55]. Natural hydrogels like GelMA are highly hydrated and porous like tissues making them a highly biocompatible choice to house cells.

#### **4.2.2 Comparison cell viability in different micro encapsulation techniques:**

Multiple studies have been done to microencapsulate different cell lines and the viability of cells was monitored over different time frames. In using laminar flow model, for cell microencapsulation Kim et.al. demonstrated that the cell viability varied in proportion to the flow rate of the oil phase [56]. In that work, the viability was observed for over seven days and on 60% of the cell population was alive [56].

Kim et al. showed the viability of encapsulated fibroblasts in GelMA using a double flow focusing microfluidic chip design. The viability was monitored for over 10 days and was up to 80%. This approach revealed that cytotoxicity of the oil used for cell microencapsulation and position of cells during encapsulation process played a key role in determining process induced damage and corresponding viability monitored over a 10 day period [56].

Weitz et al. demonstrated a 60% cell viability one day after encapsulation of microencapsulated bone marrow derived mesenchymal stem cells (BMSCs) in gelatin microspheres. Although the cells showed improved osteogenesis in vitro and in vivo in the encapsulated gelatin microspheres, the process induced damage was concerning [57][58]. The results of this work show a far better cell encapsulation density per sphere and a wider range of repeatable microspheres achieved.

Rossow et al. also demonstrated that after 1 day of encapsulation in GelMA microspheres they achieved a viability of only 60% [57] whereas the approach of the research stated in this literature demonstrates a very high cell viability of 98.03% on Day 1 indicative of minimal process induced damage.

Work done previously in the Soman lab by Sawyer et al. monitored the viability of Saos-2 cell encapsulated in 7%, 10% and 15% w/v GelMA concentrations in 5 mm GelMA macro spheres.

The viability observed was ~70% for 7% GelMA concentration, and close to ~50% for 10% and ~40% for 15% (w/v) GelMA concentrations. This is concerning because Saos-2 cells are a robust cancer cell line. If this approach were to be used to encapsulate clinically relevant stem cells which are more sensitive, a low viability would hamper successful translation for clinical tissue engineering therapy. In the discussion of their work Sawyer et al. mentioned that a low cell viability was expected as cells are encapsulated in 5 mm spheres that are beyond the diffusion limit of  $300\ \mu\text{m}$  as suggested in previous work [7][2]. A microencapsulation approach would help encapsulate cells within this suggested diffusion limit which forms the basis of the work presented in this literature.

#### **4.2.3 High sample collection efficiency and high microsphere size repeatability**

In a review by Rossow et al. problems associated with sample collection and the repeatability of the microsphere sizes are highlighted [56]. It was reported that the shear forces acting on the cells in the aqueous phase may cause process induced cell death which is a major concern. The transfer of the cell-laden micro gels into the oil phase must be as gentle as possible. This is not possible with higher flow rates and narrow device dimensions. The cytotoxic chemicals or the physical processes of pipetting used to break up emulsions can also cause cell death if the used chemicals are cytotoxic [58][57]. In this work, the channel height used is significantly taller than other designs which likely prevented high shear stress leading to low process induced damage. However, no simulation studies have been done to quantify the shear stress experienced by cells flowing through this device.

#### **4.2.4 Repeatability of the number of cells encapsulated per microsphere**

Research by multiple groups has shown that encapsulation of cells in micro gels is a stochastic process and not all generated microspheres are laden with cells[59][60][61]. It was observed that around 86 out of 100 microspheres should be empty and only 1 droplet should contain more than one cells for single cell encapsulation[59][60][61]. The statistics vary and controlling the number of cells encapsulated per microsphere, has been a pressing challenge faced by microfluidic devices designed for cell microencapsulation [59][60][61].

The system designed in this work proposes a highly flexible and customizable technique to create hydrogel droplet scaffolds that resize all parameters to help achieve enhanced cell viability. The novelty of this design allows immense flexibility in the nature of the microspheres produced. Experiments have identified a range of parameters to relate emulsion size to both experimental flow rate and solution viscosity and concentration. This design enables varying the number of cells per emulsion sphere depending on the cell density of the solution used based on the cell concentrations used.

The flexibility in choosing varying concentrations of GelMA to encapsulate cells allows control on properties like swelling and degradation of the hydrogel microspheres [62]. Also, there is control of parameters like viscosity and mechanical robustness of the used hydrogel concentrations. To support and hold the cells in place it is essential that they are seeded inside a support structure or a scaffold. Many times, cells do not get evenly seeded throughout the scaffold. The microspheres generated by this chip allow the creation of cell laden hydrogel emulsions which themselves serve as micron scale scaffolds. This can ensure adequate and even cell seeding all throughout the size of the injury or defect which needs the tissue engineered construct when a large number of these cell laden scaffolds can be injected for therapy.

This engineered chip can potentially enable micro –scale encapsulation of all clinically relevant cell types in microspheres ranging 30 to 250  $\mu\text{m}$  in size. Traditional tissue engineered constructs greater than 300 $\mu\text{m}$  in size have shown persistent challenges with oxygen and media diffusion, reflected in poor cell survival [2]. Due to the small size and range of encapsulation, effective media and oxygen diffusion is possible thereby showing enhanced cell viability. Additional procedural parameters are also controlled to ensure continued cell viability, ensuring no process-induced loss.

Rossow et.al had shown that micro encapsulation using PDMS devices fabricated using standard lithography approaches, led to microspheres 50 to 100  $\mu\text{m}$  in mean diameter in which 86 out of 100 microspheres were empty and only one microsphere should contain more than one cell [57]. The small size of our resulting GelMA microspheres opens up the possibility for multiple clinical applications. Due to the small size of achieved emulsions, they are injectable, eliminating the need for invasive surgical procedures for their application. Most constructs must be cryopreserved until their time of use, a step which strongly hinders their viability [63]. This remains a major challenge in translating these macro-scaffolds into human clinical trials. To overcome some of these limitations, micro scale encapsulation can be used. In microencapsulation, the microspheres can be simply stored in media in a well plate in an incubator as the encapsulating hydrogel itself acts as a micron scale scaffold. Most crucially, however, traditional approaches require very rigid experimental setups to achieve successful microsphere formation and subsequent cell encapsulation.

It is also observed that this micro-scale encapsulation in hydrogel makes it a lot easier to preserve these micro-scale scaffolds in a normal well plate in an incubator instead of cryopreserving the construct. As an extension of this approach as a future application, we could potentially use these injectable microspheres in an animal model to study the growth of tissue engineered constructs *in vivo* and compare results with other research groups as we have better cell density per unit microsphere volume.

### 4.3 Conclusions

Prolonged cell viability is a critical and poignant issue facing current tissue engineered constructs. This approach of cell micro encapsulation [64] using a non-clean room, 3D extrusion printing approach, serves as an inexpensive technique to make this happen. The dimensions of the microspheres allow them to be injectable and can be used as a way to avoid surgical opening up as required during implantation of other macro scale scaffolds. Even cell seeding throughout the tissue injury or defect is ensured due to the precise control over cell density as observed *in vitro*. The micro spherical shape of these cell laden constructs gives them good porosity and interconnectivity [65] when injected on top of each other. This could assist vascularization and ensure sustainability and efficient integration of the cells upon microsphere degradation. These microspheres have exhibited mechanical robustness and stability for up to 4 weeks with no visible degradation which makes them viable as scaffolds for tissue engineering applications with a potential to encapsulate clinically relevant cells. Reiterations of the experiments and viability studies have shown that this device is able to produce cell laden microspheres with minimal process induced damage. Moreover, the major advantage of this technology is the immense flexibility of experimental parameters that allows the use of all clinically relevant cell types for numerous types of tissue engineering applications. The use of 3D printing helps lower the barrier of entry to the use of microfluidic technology for other non-specific applications.



## Appendix A

### A. Supplementary Information

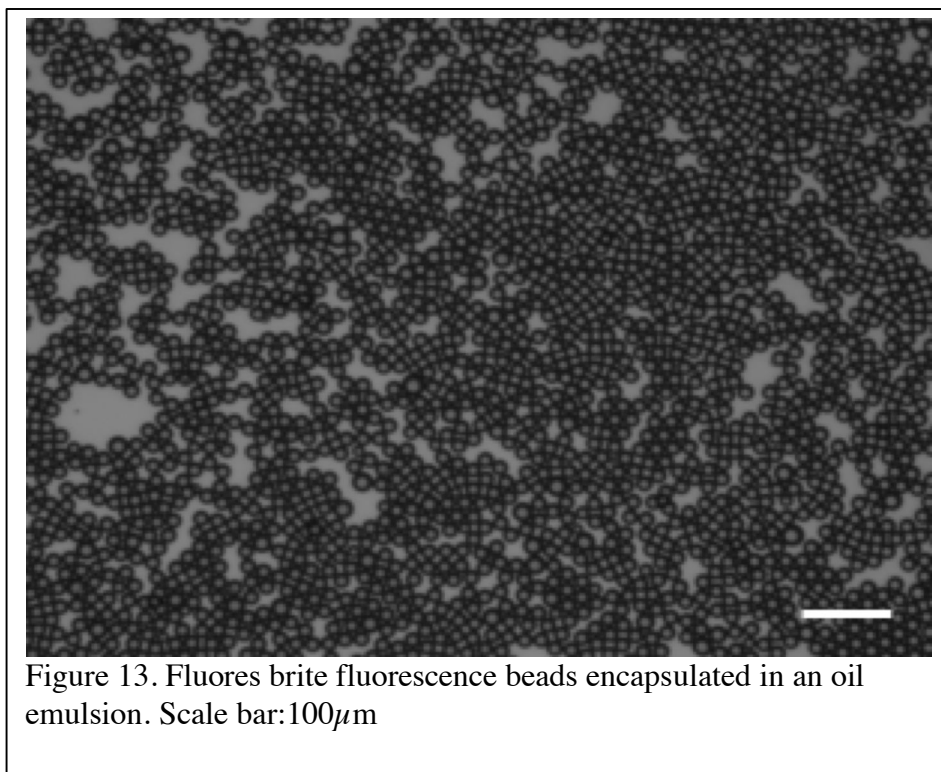
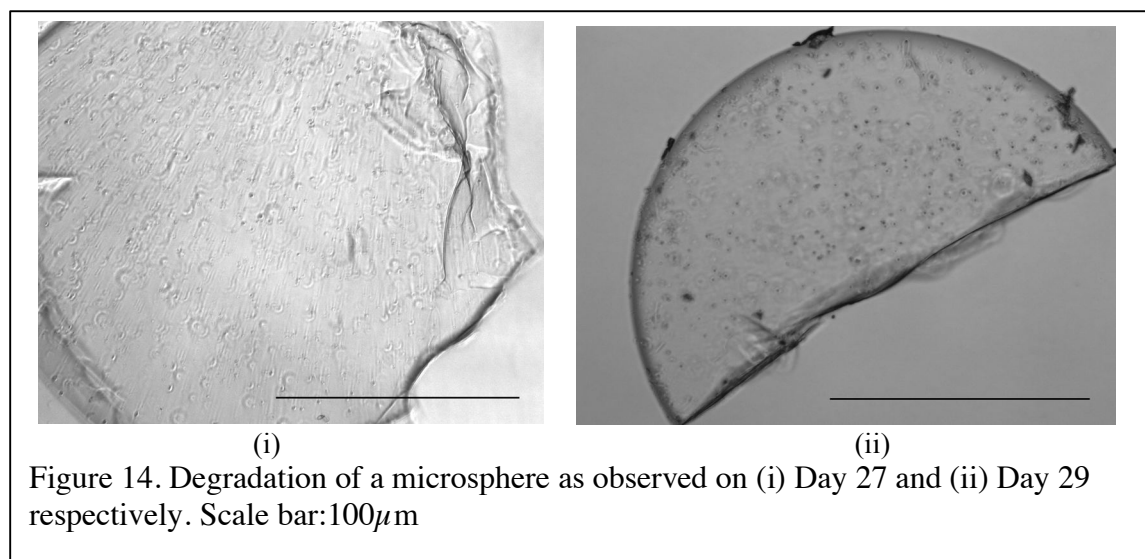


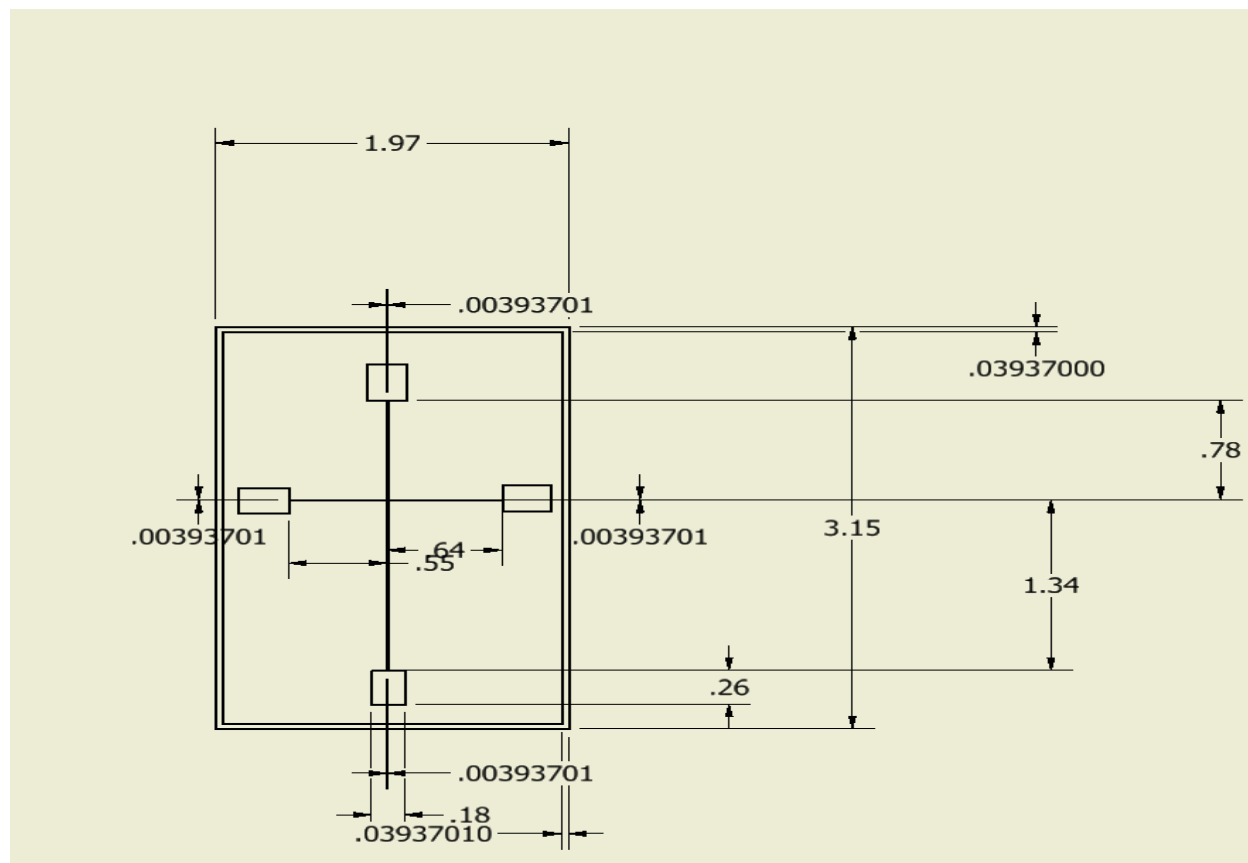
Figure 13. Fluores-brite fluorescence beads encapsulated in an oil emulsion. Scale bar: 100  $\mu\text{m}$

Figure 13 represents 10  $\mu\text{m}$  Fluores-brite YG polyethylene fluorescence micro beads encapsulated in an emulsion of perfluorodecalin oil. This was an initial primary experiment to test the chip functionality and its ability to encapsulate micron scale samples. This image was taken using an inverted fluorescence microscope at 5X. This experiment demonstrated the efficiency and range of flow rates required to achieve bead encapsulation which by extension helped me figure out how to enable cell-encapsulation going further. Figure 14 (i) and (ii) show degrading non-cell laden 100  $\mu\text{m}$  and cell laden microspheres on Day 27 and Day 29 respectively.



We took bright field images of the microspheres for day 21 and day 27 to see how much they degrade over time. The onset of considerable degradation is seen post the three-week incubation period in PBS buffer for non-cell and DMEM media for cell-laden microspheres. The microspheres stayed stable for over 3 weeks with high cell viability.

B.



Scheme 5. The sketch represents our final microfluidic chip dimensions that were used to obtain all our results consistently. The change in this device design was mainly in its channel height.

The goal of this work was to engineer a microfluidic device that can be used to engineer emulsion microsphere using a laminar flow of two immiscible phases.

C. Injection experiment with a 23-gauge needle:

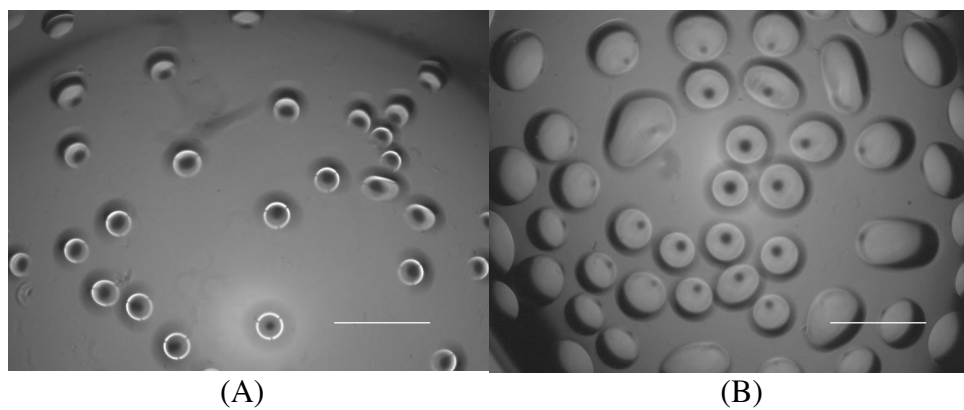


Figure 15 (A) Before and (B) After images 20x from injection of 100 $\mu$ m 8%w/v GelMA microspheres using a 23-gauge needle (Scale bar: 500 $\mu$ m)

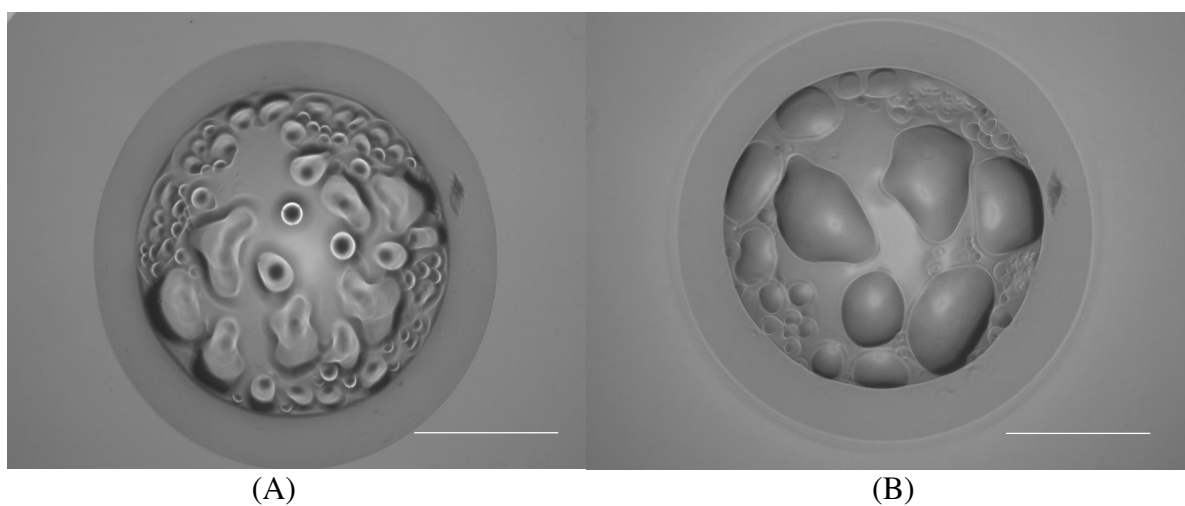


Figure 16 (A) Before and (B) After injection 5x 20 $\mu$ l emulsion of 100 $\mu$ m of 8%w/v GelMA using a 23-gauge needle (Scale bar: 500 $\mu$ m).

## D. Swelling profile data details and variations observed

Time (Minutes)	Average % Change (Size 35)	Average % Change (Size 50)	Average % Change (Size 80)	Average % Change (Size 100)	Average % Change (Size 150)
15	4.27	4.01	2.51	1.60	1.46
30	7.93	7.21	4.07	2.93	2.36
45	11.68	11.10	5.27	4.14	3.04
60	14.93	15.56	6.93	5.26	3.94
75	18.89	19.13	7.99	6.57	4.81
90	24.60	24.24	10.08	8.30	5.38
105	29.51	27.29	11.46	9.83	6.14
120	38.05	30.08	12.71	11.84	6.93
135	45.63	31.90	13.60	14.01	7.79
150	50.01	34.07	13.60	15.33	8.48
165	53.66	35.00	13.60	16.41	8.60
180	54.95	35.01	13.60	16.54	8.60
195	54.99	35.01	13.60	16.54	8.60
210	54.99	35.01	13.60	16.54	8.60
225	54.99	35.01	13.60	16.54	8.60

Table 6. Average percentage increase in mean diameter of microspheres of different sizes  
(Swelling behavior)

Time (Minutes)	Standard Deviation %Change (Size 35)	Standard Deviation %Change (Size 50)	Standard Deviation %Change (Size 80)	Standard Deviation %Change (Size 100)	Standard Deviation %Change (Size 150)
15	2.90	2.19	0.90	0.71	0.18
30	3.76	1.97	0.58	0.76	0.24
45	4.47	2.64	0.43	0.75	0.20
60	5.45	4.31	0.61	0.55	0.45
75	6.82	4.10	0.66	0.63	0.33
90	3.51	5.33	0.82	0.82	0.43
105	5.16	4.26	0.84	0.91	0.43
120	8.62	3.90	0.82	1.19	0.29
135	6.28	3.28	0.85	1.21	0.67
150	5.09	4.54	0.85	0.95	0.72

165	3.00	4.80	0.85	0.63	0.80
180	2.88	4.81	0.85	0.74	0.80
195	2.95	4.81	0.85	0.74	0.80
210	2.95	4.81	0.85	0.74	0.80
225	2.95	4.81	0.85	0.74	0.80

Table 7. Standard deviations in the corresponding percentage increase in mean sphere size observed.

E. Statistical analysis for Viability data

**Data: Percentage Viability: Within group analysis using ANOVA-one way classification**

Day 1	Day 7	Day 14	Day 21
99.3631	93.75	90.125	81.25
99.3197	93.75	90.11	81.251
99.5413	93.72	90.12	81.1457
99.5495	93.73	90.125	81.25
85.4167	93.79	90.2	81.252
99.3827	93.75	90.125	81.246
99.4398	93.75	90.125	81.25
99.5614	93.75	90.11	81.245
99.375	93.751	89.99	81.93
99.4169	93.75	90.125	81.25

Table 8. Percentage viability observed for n=10 emulsion samples for Day 1, Day 7, Day 14 and Day 21

$H_0$ : There is no significant difference between the average percentage viability with respect to time (in Days)

$H_1$ : Not  $H_0$

<b>ANOVA</b>					
Percentage Viability					
	Sum of Squares	Degrees of Freedom	Mean Square	F	p-value
Between Groups	1516.519	3	505.506	102.531	.000
Within Groups	177.491	36	4.930		
Total	1694.009	39			

Table 9. One way ANOVA analysis table

**Conclusion: Reject  $H_0$ , since p-value < 0.05 (Level of Significance). Hence, there is a significant difference between Percent Viability with respect to time (in days).**

Multiple Comparisons						
Dependent Variable: Percentage Viability						
Bonferroni Test (Pair wise Tests)						
(I) Time In Days	(J) Time In Days	Mean Difference (I-J)	Std. Error	Sig.	95% Confidence Interval	
					Lower Bound	Upper Bound
1	7	4.28751*	.99300	.001	1.5151	7.0600
	14	7.92111*	.99300	.000	5.1487	10.6936
	21	16.72964*	.99300	.000	13.9572	19.5021
7	1	-4.28751*	.99300	.001	-7.0600	-1.5151
	14	3.63360*	.99300	.005	.8612	6.4060
	21	12.44213*	.99300	.000	9.6697	15.2146
14	1	-7.92111*	.99300	.000	-10.6936	-5.1487
	7	-3.63360*	.99300	.005	-6.4060	-.8612
	21	8.80853*	.99300	.000	6.0361	11.5810
21	1	-16.72964*	.99300	.000	-19.5021	-13.9572
	7	-12.44213*	.99300	.000	-15.2146	-9.6697
	14	-8.80853*	.99300	.000	-11.5810	-6.0361
*. The mean difference is significant at the 0.05 level.						

Table 10. Bonferroni pair wise tests comparison of percentage viability as observed between different time points.

Conclusion:

1. There is a significant difference in the average percentage viability between Day1 and Day 7, Day 14 and Day 21.
2. There is a significant difference in the average percentage viability between Day 7 and Day 14 and Day 21.
3. There is a significant difference in the average percentage viability between Day 14 and Day 21.



## Bibliography

- [1] P. Bianco and P. G. Robey, "Stem cells in tissue engineering," *Nature*, vol. 414, no. 6859, p. 118, 2001.
- [2] S. W. Sawyer and M. E. Oest, "Behavior of Encapsulated Saos-2 Cells within Gelatin Methacrylate Hydrogels," *J. Tissue Sci. Eng.*, vol. 7, no. 2, 2016.
- [3] R. Kumar, M. Griffin, and P. E. Butler, "A Review of Current Regenerative Medicine Strategies that Utilize Nanotechnology to Treat Cartilage Damage," vol. 44, no. 0, pp. 862–876, 2016.
- [4] P. Bajaj, R. M. Schweller, A. Khademhosseini, J. L. West, and R. Bashir, "3D biofabrication strategies for tissue engineering and regenerative medicine," *Annu. Rev. Biomed. Eng.*, vol. 16, pp. 247–276, 2014.
- [5] A. R. Kang, J. S. Park, J. Ju, G. S. Jeong, and S. H. Lee, "Cell encapsulation via microtechnologies," *Biomaterials*, vol. 35, no. 9, pp. 2651–2663, 2014.
- [6] C. L. Murphy and A. Sambanis, "Effect of oxygen tension and alginate encapsulation on restoration of the differentiated phenotype of passaged chondrocytes," *Tissue Eng.*, vol. 7, no. 6, pp. 791–803, 2001.
- [7] U. Schloßmacher *et al.*, "Alginate/silica composite hydrogel as a potential morphogenetically active scaffold for three-dimensional tissue engineering," *RSC Adv.*, vol. 3, no. 28, pp. 11185–11194, 2013.
- [8] W. Jiang, M. Li, Z. Chen, and K. W. Leong, "Lab on a Chip," *Lab Chip*, vol. 16, pp. 4482–4506, 2016.
- [9] S. V. Murphy and A. Atala, "3D bioprinting of tissues and organs," *Nat. Biotechnol.*, vol. 32, no. 8, pp. 773–785, 2014.
- [10] X. Zhao, S. Liu, L. Yildirim, H. Zhao, R. Ding, and H. Wang, "Injectable Stem Cell-Laden Photocrosslinkable Microspheres Fabricated Using Microfluidics for Rapid Generation of Osteogenic Tissue Constructs," pp. 2809–2819, 2016.
- [11] N. Kashyap, N. Kumar, and M. N. V. R. Kumar, "Hydrogels for pharmaceutical and biomedical applications," *Crit. Rev. Ther. Drug Carr. Syst.*, vol. 22, no. 2, 2005.
- [12] H. Black, "Tiny technology promises tremendous profits: by reducing volumes of expensive chemicals and reagents, microfluidics may offer cost advantages for testing drugs and processes.(Profession)," *Sci.*, vol. 15, no. 21, pp. 29–31, 2001.
- [13] A. Murua, A. Portero, G. Orive, R. M. Hernández, M. de Castro, and J. L. Pedraz, "Cell microencapsulation technology: towards clinical application," *J. Control. Release*, vol. 132, no. 2, pp. 76–83, 2008.
- [14] M. Stjernström and J. Roeraade, "Method for fabrication of microfluidic systems in glass," *J. Micromechanics Microengineering*, vol. 8, no. 1, p. 33, 1998.
- [15] M. W. Losey, R. J. Jackman, S. L. Firebaugh, M. A. Schmidt, and K. F. Jensen, "Design and fabrication of microfluidic devices for multiphase mixing and reaction," *J. Microelectromechanical Syst.*, vol. 11, no. 6, pp. 709–717, 2002.
- [16] G. Velte-Casquillas, M. Le Berre, M. Piel, and P. T. Tran, "Microfluidic tools for cell biological research," *Nano Today*, vol. 5, no. 1, pp. 28–47, 2010.
- [17] S.-Y. Teh, R. Lin, L.-H. Hung, and A. P. Lee, "Droplet microfluidics," *Lab Chip*, vol. 8, no. 2, pp. 198–220, 2008.
- [18] D. M. Headen, G. Aubry, H. Lu, and A. J. García, "Microfluidic-based generation of size-controlled, biofunctionalized synthetic polymer microgels for cell encapsulation," *Adv.*

- Mater.*, vol. 26, no. 19, pp. 3003–3008, 2014.
- [19] P. Garstecki, M. J. Fuerstman, H. A. Stone, and G. M. Whitesides, “Formation of droplets and bubbles in a microfluidic T-junction—scaling and mechanism of break-up,” *Lab Chip*, vol. 6, no. 3, pp. 437–446, 2006.
  - [20] M. Chabert and J.-L. Viovy, “Microfluidic high-throughput encapsulation and hydrodynamic self-sorting of single cells,” *Proc. Natl. Acad. Sci.*, vol. 105, no. 9, pp. 3191–3196, 2008.
  - [21] H. Becker and L. E. Locascio, “Polymer microfluidic devices,” *Talanta*, vol. 56, no. 2, pp. 267–287, 2002.
  - [22] T. Ito and S. Okazaki, “Pushing the limits of lithography,” *Nature*, vol. 406, no. 6799, p. 1027, 2000.
  - [23] R. S. Kane, S. Takayama, E. Ostuni, D. E. Ingber, and G. M. Whitesides, “Patterning proteins and cells using soft lithography,” *Biomaterials*, vol. 20, no. 23, pp. 2363–2376, 1999.
  - [24] C. Iliescu, H. Taylor, M. Avram, J. Miao, and S. Franssila, “A practical guide for the fabrication of microfluidic devices using glass and silicon,” *Biomicrofluidics*, vol. 6, no. 1, p. 16505, 2012.
  - [25] J. L. Liow, “Mechanical micromachining: a sustainable micro-device manufacturing approach?,” *J. Clean. Prod.*, vol. 17, no. 7, pp. 662–667, 2009.
  - [26] L. Peng, Y. Deng, P. Yi, and X. Lai, “Micro hot embossing of thermoplastic polymers: a review,” *J. Micromechanics Microengineering*, vol. 24, no. 1, p. 13001, 2013.
  - [27] S. Koo, S. M. Santoni, B. Z. Gao, C. P. Grigoropoulos, and Z. Ma, “Laser-assisted biofabrication in tissue engineering and regenerative medicine,” *J. Mater. Res.*, vol. 32, no. 1, pp. 128–142, 2017.
  - [28] D. Qin, Y. Xia, and G. M. Whitesides, “Soft lithography for micro- and nanoscale patterning,” *Nat. Protoc.*, vol. 5, no. 3, p. 491, 2010.
  - [29] U. M. Attia, S. Marson, and J. R. Alcock, “Micro-injection moulding of polymer microfluidic devices,” *Microfluid. Nanofluidics*, vol. 7, no. 1, p. 1, 2009.
  - [30] A. Manuscript, “NIH Public Access,” vol. 4, no. 3, pp. 1–25, 2013.
  - [31] G. D. Nicodemus and S. J. Bryant, “Cell encapsulation in biodegradable hydrogels for tissue engineering applications,” *Tissue Eng. Part B Rev.*, vol. 14, no. 2, pp. 149–165, 2008.
  - [32] C. G. Williams, A. N. Malik, T. K. Kim, P. N. Manson, and J. H. Elisseeff, “Variable cytocompatibility of six cell lines with photoinitiators used for polymerizing hydrogels and cell encapsulation,” *Biomaterials*, vol. 26, no. 11, pp. 1211–1218, 2005.
  - [33] H. Becker and C. Gärtner, “Polymer microfabrication technologies for microfluidic systems,” *Anal. Bioanal. Chem.*, vol. 390, no. 1, pp. 89–111, 2008.
  - [34] K. Yue, G. Trujillo-de Santiago, M. M. Alvarez, A. Tamayol, N. Annabi, and A. Khademhosseini, “Synthesis, properties, and biomedical applications of gelatin methacryloyl (GelMA) hydrogels,” *Biomaterials*, vol. 73, pp. 254–271, 2015.
  - [35] Stratasys, “No Title,” 2017. [Online]. Available: <http://www.stratasys.com/3d-printers/objet30-pro>.
  - [36] M. A. Eddings, M. A. Johnson, and B. K. Gale, “Determining the optimal PDMS–PDMS bonding technique for microfluidic devices,” *J. Micromechanics Microengineering*, vol. 18, no. 6, p. 67001, 2008.
  - [37] F. Tamimi *et al.*, “Perfluorodecalin and bone regeneration,” vol. 25, pp. 22–36, 2013.

- [38] E. Leclerc, Y. Sakai, and T. Fujii, "Cell culture in 3-dimensional microfluidic structure of PDMS (polydimethylsiloxane)," *Biomed. Microdevices*, vol. 5, no. 2, pp. 109–114, 2003.
- [39] C.-H. Choi, J.-H. Jung, Y. W. Rhee, D.-P. Kim, S.-E. Shim, and C.-S. Lee, "Generation of monodisperse alginate microbeads and in situ encapsulation of cell in microfluidic device," *Biomed. Microdevices*, vol. 9, no. 6, pp. 855–862, 2007.
- [40] A. I. Van Den Bulcke, B. Bogdanov, N. De Rooze, E. H. Schacht, M. Cornelissen, and H. Berghmans, "Structural and rheological properties of methacrylamide modified gelatin hydrogels," *Biomacromolecules*, vol. 1, no. 1, pp. 31–38, 2000.
- [41] S. B. Rodan *et al.*, "Characterization of a human osteosarcoma cell line (Saos-2) with osteoblastic properties," *Cancer Res.*, vol. 47, no. 18, pp. 4961–4966, 1987.
- [42] G. K. Naughton, "lab bench to market: critical issues in tissue engineering," *Ann. N. Y. Acad. Sci.*, vol. 961, pp. 372–385, 2002.
- [43] G. Vunjak-Novakovic, B. Obradovic, I. Martin, P. M. Bursac, R. Langer, and L. E. Freed, "Dynamic cell seeding of polymer scaffolds for cartilage tissue engineering," *Biotechnol. Prog.*, vol. 14, no. 2, pp. 193–202, 1998.
- [44] P. Coimbra, D. Fernandes, P. Ferreira, M. H. Gil, and H. C. de Sousa, "Solubility of Irgacure® 2959 photoinitiator in supercritical carbon dioxide: Experimental determination and correlation," *J. Supercrit. Fluids*, vol. 45, no. 3, pp. 272–281, 2008.
- [45] Y. Ling *et al.*, "A cell-laden microfluidic hydrogel," *Lab Chip*, vol. 7, no. 6, pp. 756–762, 2007.
- [46] C. M. B. Ho, S. H. Ng, K. H. H. Li, and Y.-J. Yoon, "3D printed microfluidics for biological applications," *Lab Chip*, vol. 15, no. 18, pp. 3627–3637, 2015.
- [47] A. Folch, A. Ayon, O. Hurtado, M. A. Schmidt, and M. Toner, "Molding of deep polydimethylsiloxane microstructures for microfluidics and biological applications," *J. Biomech. Eng.*, vol. 121, no. 1, pp. 28–34, 1999.
- [48] N. Bhattacharjee, A. Urrios, S. Kang, and A. Folch, "The upcoming 3D-printing revolution in microfluidics," *Lab Chip*, vol. 16, no. 10, pp. 1720–1742, 2016.
- [49] D. C. Duffy, J. C. McDonald, O. J. A. Schueller, and G. M. Whitesides, "Rapid prototyping of microfluidic systems in poly (dimethylsiloxane)," *Anal. Chem.*, vol. 70, no. 23, pp. 4974–4984, 1998.
- [50] G. S. Fiorini and D. T. Chiu, "Disposable microfluidic devices: fabrication, function, and application," *Biotechniques*, vol. 38, no. 3, pp. 429–450, 2005.
- [51] A. K. Au, W. Huynh, L. F. Horowitz, and A. Folch, "3D-printed microfluidics," *Angew. Chemie Int. Ed.*, vol. 55, no. 12, pp. 3862–3881, 2016.
- [52] K. Willis, E. Brockmeyer, S. Hudson, and I. Poupyrev, "Printed optics: 3D printing of embedded optical elements for interactive devices," in *Proceedings of the 25th annual ACM symposium on User interface software and technology*, 2012, pp. 589–598.
- [53] S. Waheed *et al.*, "3D printed microfluidic devices: enablers and barriers," *Lab Chip*, vol. 16, no. 11, pp. 1993–2013, 2016.
- [54] H. Wang *et al.*, "Cell-laden photocrosslinked GelMA–DexMA copolymer hydrogels with tunable mechanical properties for tissue engineering," *J. Mater. Sci. Mater. Med.*, vol. 25, no. 9, pp. 2173–2183, 2014.
- [55] R. L. Whistler, "Hydrogels-synthetic and natural," *J. Tech. Assoc. Pulp Pap. Ind.*, vol. 60, no. 12, pp. 64–67, 1977.
- [56] S. Kim, J. Oh, and C. Cha, "Colloids and Surfaces B : Biointerfaces Enhancing the biocompatibility of microfluidics-assisted fabrication of cell-laden microgels with channel

- geometry,” *Colloids Surfaces B Biointerfaces*, vol. 147, pp. 1–8, 2016.
- [57] T. Rossow, P. S. Lienemann, and D. J. Mooney, “Cell Microencapsulation by Droplet Microfluidic Templating,” vol. 1600380, pp. 1–14, 2016.
  - [58] X. Zhao *et al.*, “Injectable Stem Cell-Laden Photocrosslinkable Microspheres Fabricated Using Microfluidics for Rapid Generation of Osteogenic Tissue Constructs,” *Adv. Funct. Mater.*, vol. 26, no. 17, pp. 2809–2819, 2016.
  - [59] S. Utech, R. Prodanovic, A. S. Mao, R. Ostafe, D. J. Mooney, and D. A. Weitz, “Microfluidic generation of monodisperse, structurally homogeneous alginate microgels for cell encapsulation and 3D cell culture,” *Adv. Healthc. Mater.*, vol. 4, no. 11, pp. 1628–1633, 2015.
  - [60] S. Köster *et al.*, “Drop-based microfluidic devices for encapsulation of single cells,” *Lab Chip*, vol. 8, no. 7, pp. 1110–1115, 2008.
  - [61] Y. Ma, M. P. Neubauer, J. Thiele, A. Fery, and W. T. S. Huck, “Artificial microniches for probing mesenchymal stem cell fate in 3D,” *Biomater. Sci.*, vol. 2, no. 11, pp. 1661–1671, 2014.
  - [62] J. W. Nichol, S. T. Koshy, H. Bae, C. M. Hwang, S. Yamanlar, and A. Khademhosseini, “Cell-laden microengineered gelatin methacrylate hydrogels,” *Biomaterials*, vol. 31, no. 21, pp. 5536–5544, 2010.
  - [63] M. D. Kofron, N. C. Opsitnick, M. A. Attawia, and C. T. Laurencin, “Cryopreservation of tissue engineered constructs for bone,” *J. Orthop. Res.*, vol. 21, no. 6, pp. 1005–1010, 2003.
  - [64] G. Orive *et al.*, “History, challenges and perspectives of cell microencapsulation,” *TRENDS Biotechnol.*, vol. 22, no. 2, pp. 87–92, 2004.
  - [65] Q. L. Loh and C. Choong, “Three-dimensional scaffolds for tissue engineering applications: role of porosity and pore size,” *Tissue Eng. Part B Rev.*, vol. 19, no. 6, pp. 485–502, 2013.

**VITA**

**NAME OF AUTHOR:** Sanika Suvarnapathaki

**PLACE OF BIRTH:** Thane, India

**DATE OF BIRTH:** December 25,1993

**EDUCATION:**

B.E. Biomedical Engineering, University of Mumbai, India (2015).

MS BIOENGINEERING, SYRACUSE UNIVERSITY, NEW YORK, USA (2015-PRESENT).